

DIFFERENTIAL CROSS SECTIONS FOR CHARGE
TRANSFER USING SCREENED COULOMB POTENTIALS
IN THE EIKONAL APPROXIMATION

by

STEVEN RAY ROGERS

B.A., University of Northern Colorado, 1975

A MASTER'S THESIS

submitted in partial fulfillment of the

requirements for the degree

MASTER OF SCIENCE


Department of Physics

KANSAS STATE UNIVERSITY

Manhattan, Kansas

1977

Approved by:


Major Professor

Document

LD

2668

T4

1977

R65

C.2

TABLE OF CONTENTS

LIST OF FIGURES.	11
ACKNOWLEDGMENTS.	iii
CHAPTER 1. INTRODUCTION	1
CHAPTER 2. THEORY	9
SECTION 2.1 The Differential Cross Section.	9
SECTION 2.2 The Hamiltonian	11
SECTION 2.3 The Eikonal Phase	13
SECTION 2.4 The Eikonal Impact Parameter Method	15
CHAPTER 3. APPLICATIONS AND RESULTS	18
SECTION 3.1 The Static Brinkman-Kramers Approximation	18
SECTION 3.2 The Screened Coulomb Brinkman-Kramers Approximation	21
SECTION 3.3 Protons on Hydrogen	22
SECTION 3.4 Protons on Helium	27
SECTION 3.5 Protons on Argon.	33
CHAPTER 4. CONCLUSION	36
REFERENCES	38
APPENDIX 1	40
APPENDIX 2	48
APPENDIX 3	54
APPENDIX 4	68
ABSTRACT	76

LIST OF FIGURES

Figure 1.	Scattering of an ion from an atomic target.	3
Figure 2.	Differential cross section for capture of K-shell elec- trons from argon by 6 MeV protons	7
Figure 3.	The differential cross section for 50 keV protons inci- dent on atomic hydrogen	25
Figure 4.	Differential cross section for capture of K-shell elec- trons from helium by 293 keV protons.	29
Figure 5.	The laboratory angle $\theta_{1/2}$ where the scattering distribution falls to half the maximum intensity as a function of pro- jectile energy.	32
Figure 6.	Differential cross section for capture of K-shell elec- trons from argon by 6 MeV protons	35
Figure 7.	The coordinates for the charge transfer process $A +$ $(e + B) \rightarrow (A + e) + B$	42

ACKNOWLEDGMENTS

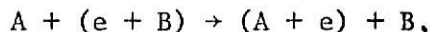
I would like to thank the Kansas State University physics department for the support of their graduates through teaching and research assistantships. I am indebted to many of the Kansas State University professors for freely sharing their love and knowledge in physics. I am deeply indebted to Jim McGuire for his helpful advice both as a friend and major professor. I would like to give a special thanks to Jolea Hay who meticulously typed this thesis.

I would like to dedicate this work to my mother who has labored to provide me with my education. And most importantly, I would like to thank my loving wife who has provided for my health and emotional well being and shares with me in a dream.

CHAPTER 1

INTRODUCTION

Charge transfer or, sometimes, electron capture is a type of rearrangement collision. This is depicted in the reaction,



where A represents the projectile system, B the target system, and e the transferred electron. Due to the Coulomb interactions influencing the projectile's path, the projectile will scatter at various angles depending on the impact parameter, see Figure 1. Looking at many scattering events corresponding to various impact parameters, an angular distribution will arise. Calculation of the charge transfer angular distributions from the K shell by proton impact is presented in this thesis.

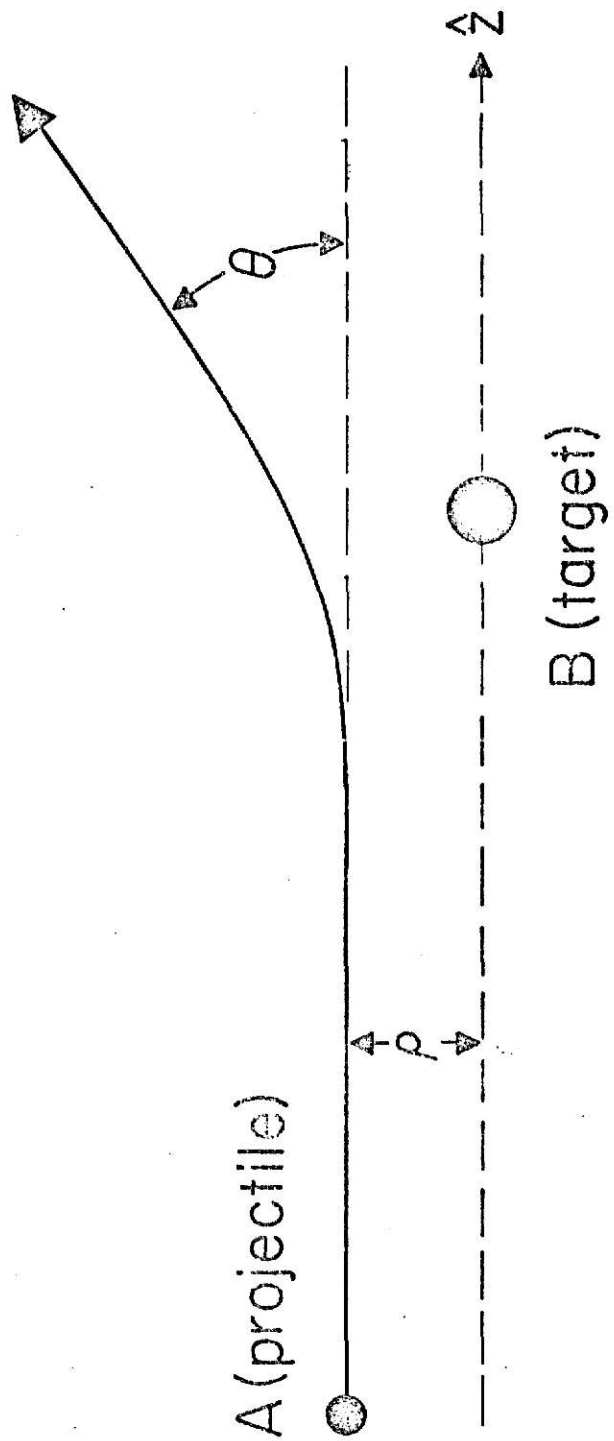
Thus far, charge transfer calculations yield non rigorous total cross sections for K shell capture. The most extensively used method for determining electron capture cross sections is the first Born approximation or, simply, the Born approximation. This method is used for its simplicity and not necessarily for its validity. It is known that the second Born term dominates at very high energies¹ and second order calculations are now being pursued. In this presentation, the simplicity of the first order calculation is retained while viewing the differential cross section for charge transfer.

Examination of the differential cross section can give a deeper understanding of the charge transfer process. The perturbing potential for charge transfer is still somewhat unclear. Since the differential

**THIS BOOK
CONTAINS
NUMEROUS PAGES
THAT WERE
BOUND WITHOUT
PAGE NUMBERS.**

**THIS IS AS
RECEIVED FROM
CUSTOMER.**

Figure 1. Scattering of an ion from an atomic target, where ρ is the impact parameter and θ is the scattering angle.



cross section is sensitive to how the Hamiltonian is broken up, detailed information of the charge transfer process is possible. Thus, calculations of angular distributions could lend credence to ideas as to how the Hamiltonian for charge transfer should be broken up in first order perturbation theory.

One of the first charge transfer calculations was done by Brinkman and Kramers² in 1930. Their calculation was performed adhering to the point of view that the relevant interaction potential was between the projectile and (captured) electron³. It is argued that the internuclear interaction, which is largely responsible for the path of the projectile, contributes little to the total capture cross section for heavy particles. For most capture cross sections, the resulting BK total cross sections were typically too large by a factor⁴ of 2 to 10.

Another first order calculation was performed by Jackson and Schiff⁵ in 1953 for the special case of protons incident upon hydrogen. The potential used in the JS calculation was the full interaction, that is, the BK potential and the internuclear (or core) potential. Including the "core" term had the effect of reducing the total cross section over a range of energies thus giving much better agreement with experiment. However, when the JS method was applied to other systems of higher nuclear charge, total calculated cross sections were found to disagree with experiment by as much as several orders of magnitude.^{6,7}

The success of the JS approach was later partially explained by Bates⁸ in 1958. Taking into account the nonorthogonality of the initial and final state wave functions, Bates was able to demonstrate that a JS like core term with unit nuclear charge originates from the average electron interaction. This tends to account for the relative success of the

JS method for protons on hydrogen, and suggests an alternate method for targets of nuclear charge greater than one.

At the present time, some believe that the Bates calculation offers the most complete picture for viewing charge transfer to first order. Nevertheless, only various approximations for the Bates method of charge exchange have been used resulting in total cross sections that tend to agree with experiment.^{9,10} The success of these approximations in predicting total cross sections tend to indicate that the Bates approach is superior to that of BK or JS.

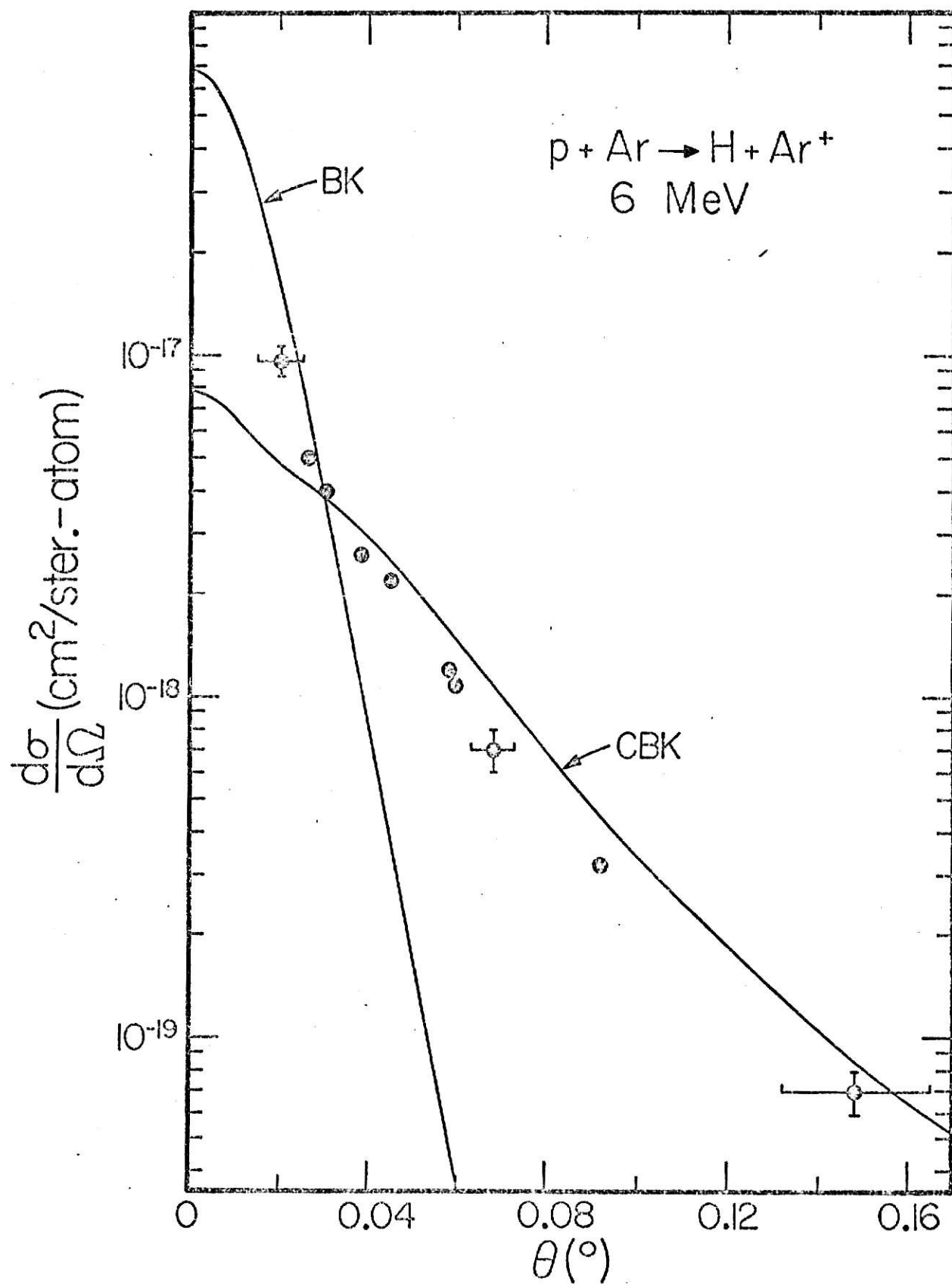
Taking advantage of the heavy projectile mass, it is often useful to study the charge transfer process by means of the impact parameter treatment. A transformation from the wave picture over to an impact parameter picture is presented in appendix 1. This impact parameter formalism was used by Belkic and Salin¹¹ in 1976 for the angular distributions for charge transfer.

The impact parameter formalism used in Belkic and Salin's calculation employs an eikonal phase so as to include the internuclear potential together with the Brinkman-Kramers method. Justification for the use of the eikonal phase within the impact parameter treatment is made in Chapter 2. By including the internuclear potential in the eikonal phase, Belkic and Salin were able to get improved agreement at wide angles with the differential cross section for electron capture from argon by 6 MeV protons observed by Cocke,¹² et al., in 1976, see Figure 2. Using the BK probability amplitude for capture which is calculated in a straight-line impact-parameter version of the BK approximation Belkic and Salin were able to obtain a better angular distribution than the BK calculation which took into account no contributions of the internuclear repulsion.

Figure 2. Differential cross section in laboratory system for capture of K-shell electrons from argon by 6 MeV protons. The curve marked BK represents the Brinkman-Kramers approximation; and CBK, the Coulomb Brinkman-Kramers approximation. Experimental data are those of Cocke, et al., (1976). Figure taken from Belkic and Salin, J. Phys. B: Atom. Molec. Phys. 9, L397 (1976).

**THIS BOOK
CONTAINS
NUMEROUS PAGES
WITH DIAGRAMS
THAT ARE CROOKED
COMPARED TO THE
REST OF THE
INFORMATION ON
THE PAGE.**

**THIS IS AS
RECEIVED FROM
CUSTOMER.**



**THIS BOOK
CONTAINS
NUMEROUS PAGES
WITH THE ORIGINAL
PRINTING BEING
SKEWED
DIFFERENTLY FROM
THE TOP OF THE
PAGE TO THE
BOTTOM.**

**THIS IS AS RECEIVED
FROM THE
CUSTOMER.**

Note that their results are in good agreement at large angles (i.e. small impact parameters) but may give poor agreement at the forward angles (i.e. large impact parameters). Data for protons on helium support this trend, suggesting that the scattering potential is too strong at large impact parameters.

One of the limitations of the Belkic and Salin calculation is the omission of the screening effects by the electrons at large impact parameters. We include the effects of screening by the electrons in an approximate manner. For $p + H$ and $p + He$, the internuclear potential is represented by the static potential (cf. Chapter 2) which is introduced into the eikonal phase within the BK method. Hence, it will be referred to as the Static Brinkman-Kramers (SBK) approximation. For $p + Ar$ which is mathematically more complex, a screened Coulomb potential is incorporated in the eikonal phase as an approximation for the static potential. This Screened Coulomb Brinkman-Kramers calculation will be referred to as the SCBK approximation.

Application of the eikonal impact parameter treatment of charge transfer is made for three specific cases. The relatively simple system of protons incident upon hydrogen is presented first. This is followed by protons incident on helium. Then finally, the more complex system of protons on argon is examined. The two later cases are compared with recently gathered experimental differential cross sections for charge transfer.

CHAPTER 2

THEORY

2.1 The Differential Cross Section

The differential cross section is defined as

$$\frac{d\sigma}{d\Omega} = \frac{\text{Number of particles per unit time scattered into a solid angle}}{\text{Number of particles incident on the target per unit area per unit time}}.$$

This can be written symbolically as,

$$\frac{d\sigma}{d\Omega} = \frac{\omega/d\Omega_f}{I}. \quad (2.1)$$

The incident flux, I , can be given as,

$$\begin{aligned} I &= \frac{\text{velocity of incident particle}}{\text{unit volume}} \\ &= \frac{k_i \hbar}{\mu_i L^3} \end{aligned} \quad (2.2)$$

where $\hbar k_i$ is the magnitude of the relative initial momentum, μ_i is the initial reduced mass of the system, and L^3 is the volume of a cube of length, L . The transition probability per unit time, ω , is given by,

$$\omega = \frac{2\pi}{\hbar} \rho_f |\langle \phi_f | H' | \Psi \rangle|^2, \quad (2.3)$$

where ρ_f is the density of final states and $\langle \phi_f | H' | \Psi \rangle$ is the transition matrix element for a transition from all possible states, Ψ , into the

final state, ϕ_f , under the perturbing Hamiltonian, H' . The density of final states, ρ_f , is given by,

$$\rho_f = \frac{\mu_f k_f d\Omega_f L^3}{(2\pi)^3 \hbar^2}, \quad (2.4)$$

where μ_f is the reduced mass of the final system, $\hbar k_f$ is the magnitude of the final relative momentum, $d\Omega_f$ is the solid angle subtended by the detector, and L^3 is the volume. Combining eq. 2.1, 2.2, 2.3 and 2.4, the differential cross section becomes,

$$\frac{d\sigma}{d\Omega} = \frac{\mu_i \mu_f L^6}{(2\pi)^2 \hbar^4} \left(\frac{k_f}{k_i} \right) |\langle \phi_f | H' | \psi \rangle|^2 \quad (2.5)$$

It is now convenient to introduce atomic units ($e^2 = \hbar = m_e = 1$), where e is the electron charge and m_e is the electron mass. A few basic units are given below;

$$\text{unit length} = a_0 = \frac{\hbar^2}{m_e e^2} = 5.29 \cdot 10^{-9} \text{ cm}$$

$$\text{unit energy} = \frac{m_e e^4}{\hbar^2} = 27.2 \text{ eV}$$

$$\text{unit time} = \frac{\hbar^3}{m_e e^4} = 2.42 \cdot 10^{-17} \text{ sec.}$$

Atomic units will be used unless stated otherwise.

The differential cross section given in atomic units is,

$$\frac{d\sigma}{d\Omega} = \frac{\mu_i \mu_f}{(2\pi)^2} \left(\frac{k_f}{k_i} \right) |\langle \phi_f | H' | \psi \rangle|^2, \quad (2.6)$$

where the wave functions are normalized to the unit volume, L^3 . As yet, all we have done is to have re-written the definition of differential cross section into a form that can be used for calculation.

2.2 The Hamiltonian

Charge transfer is not a well understood atomic process. In our quest toward understanding the charge transfer process, approximations for both the wave functions and the perturbing Hamiltonian are made. However, in making approximations for the wave functions, difficulties arise from the fact that the wave functions are not described in the same basis set (i.e., nonorthogonal wave functions are used). In addition, it is a general practice to consider only one electron target atoms in charge transfer.

The Hamiltonian for a charged projectile incident upon a multi-electron target (assuming two body interactions) is given by,

$$\begin{aligned}
 H &= \text{Total Kinetic Energy} + \text{Total Potential Energy} \\
 &= \frac{P_a^2}{2M_a} + \frac{Z_a Z_b e^2}{R} - \sum_{j=1}^{Z_b} \frac{Z_a e^2}{|\vec{R} - \vec{r}_j|} \\
 &\quad + \sum_{j=1}^{Z_b} \left(\frac{P_j^2}{2m_e} - \frac{Z_b e^2}{r_i} \right) + \sum_{k>j}^{Z_b} \frac{e^2}{|\vec{r}_k - \vec{r}_j|} \quad (2.7)
 \end{aligned}$$

where Z_a and M_a are the charge and mass of the incident projectile with momentum P , Z_b is the charge of the target nucleus, R represents the projectile coordinate and $\vec{r}_1 \dots \vec{r}_{Z_b}$ the set of coordinates of the target electrons measured from the target nucleus, and P_j is the momentum of the j th electron. By adding then subtracting the average projectile electron potential (i.e.,

$$\bar{V}_e^j \equiv \langle \phi_i | \frac{-Z_a e^2}{|\vec{R} - \vec{r}_j|} | \phi_i \rangle \quad (2.8)$$

where ϕ_i is the initial bound state wave function for the j th electron), the Hamiltonian in eq. 2.7 takes the form,

$$H \equiv \frac{P_a^2}{2M_a} + V_s(R) + H' + H'_o + H_o, \quad (2.9)$$

where $V_s(R)$ is the static potential¹⁵ given by

$$V_s(R) \equiv \frac{Z_a Z_b e^2}{R} + \sum_{j=1}^{Z_b} \bar{V}_e^j \quad (2.10)$$

or

$$V_s(R) \equiv Z_a \left[\frac{Z_b e^2}{R} + \sum_{j=1}^{Z_b} \frac{\rho(\vec{r}_j)}{|\vec{R} - \vec{r}_j|} d\vec{r}_j \right],$$

where $\rho(\vec{r}_j)$ is the charge density for the j th electron H' is the electron capture potential prescribed by Bates,⁸ i.e.,

$$H' \equiv \frac{-Z_a e^2}{|\vec{R} - \vec{x}|} + \langle \phi_i | \frac{Z_a e^2}{|\vec{R} - \vec{x}|} | \phi_i \rangle \quad (2.11)$$

where \vec{x} is the coordinate of the captured electron measured from the target nucleus; H'_o is the Hamiltonian that describes the initial bound state of the electron to be captured, i.e.,

$$H'_o \equiv \frac{P_e^2}{2m_e} - \frac{Z_b e^2}{x} + V(\vec{x}), \quad (2.11A)$$

where P_e is the momentum of the captured electron and $V(\vec{x})$ is the effective potential between the captured electron and the spectator electrons, i.e.,

$$V(\vec{x}) \approx \sum_{k=1}^{Z_b} \frac{e^2}{|\vec{r}_k - \vec{x}|}, \quad (2.11B)$$

where the prime indicates the restricted sum $r_k \neq x$; and H_0 is the Hamiltonian for the spectator electrons which is given by

$$H_0 \equiv \sum_{j=1}^{Z_b-1} \left[\frac{p_j^2}{2m_e} - \frac{Z_b e^2}{r_j} + V(\vec{r}_j) - \bar{v}_e^j \right], \quad (2.11C)$$

where the summation is over all the spectator electrons and $V(\vec{r}_j)$ is the effective potential between the spectator electrons (cf. eq. 2.11B). To retain the simplicity of the one electron atom, the effects due to the spectator electrons, eq. 2.11C, are ignored¹⁴ in the development to follow. This is done so that simple hydrogenic wave functions can be used to describe the bound state of the captured electron. Note that in this fashion of breaking up the Hamiltonian, both the static potential and the electron capture potential of Bates are directly related.

The perturbation to the one electron Hamiltonian is separable into two categories: the perturbation for electron capture and the perturbation responsible for scattering of the projectile. Both are needed for the differential cross section. The perturbation for the capture process is the Bates potential, eq. 2.11. The "scattering" perturbation is the static potential given by eq. 2.10. We choose to treat these two processes separately.

2.3 The Eikonal Phase

We can treat the scattering process within the eikonal approximation. As an introduction to the eikonal approximation, let us consider the scattering of a particle from the central potential, $V(R)$. The time

independent Schrödinger equation for such a process is

$$\left(-\frac{\nabla^2}{2\mu} + V(R) \right) \psi = \frac{k^2}{2\mu} \psi, \quad (2.12)$$

where μ is the reduced mass and k is the momentum of the projectile.

Assuming our wave function to be of the form,

$$\psi = e^{i\vec{k} \cdot \vec{R}} \phi(R) \quad (2.13)$$

and substituting into eq. 2.12 we get

$$\left(\frac{k^2}{2\mu} \phi(R) - \frac{\nabla^2}{2\mu} \phi(R) - \frac{2i\vec{k} \cdot \vec{\nabla} \phi(R)}{2\mu} + V(R) \phi(R) \right) \times e^{i\vec{k} \cdot \vec{R}} = \frac{k^2}{2\mu} \phi(R) e^{i\vec{k} \cdot \vec{R}}. \quad (2.14)$$

Equation 2.14 reduces to

$$-\frac{\nabla^2}{2\mu} \phi(R) - \frac{i\vec{k} \cdot \vec{\nabla} \phi(R)}{\mu} + V(R) \phi(R) = 0. \quad (2.15)$$

Assuming $\phi(R)$ to vary slowly over many wavelengths of the incident projectile,¹⁶ i.e.

$$\nabla^2 \phi(R) \ll \vec{k} \cdot \vec{\nabla} \phi(R), \quad (2.16)$$

choosing \vec{k} along the z direction, and solving eq. 2.15 for $\phi(R)$ we get

$$\phi(R) = \left[\exp \frac{-\mu i}{k} \int_{-\infty}^{\infty} V(R) dz \right]. \quad (2.17)$$

Noting that $R = \sqrt{\rho^2 + z^2}$ where ρ is the impact parameter, our projectile

wave function (eq. 2.13) is

$$\psi \approx \exp(i\vec{k}_i \cdot \vec{R}_i + 2i\delta(\rho)), \quad (2.18)$$

where

$$\delta(\rho) \equiv -\frac{1}{v} \int_0^\infty V(R) dz, \quad (2.19)$$

and $\mu v = k$.

2.4 The Eikonal Impact Parameter Method

McCarroll and Salin¹⁷ (1968) present a method for evaluation of the differential cross section (Appendix 1) where the wave picture is formally transformed into an impact parameter picture. The results of this method were then modified by Belkic and Salin (1976) so as to include scattering from the internuclear potential in an eikonal phase. The internuclear potential used by Belkic and Salin appears to be too strong at the large impact parameters which suggests that screening of the electrons is important for angular distributions. Here the eikonal impact parameter method used by Belkic and Salin is presented in a general form so that the screening effects are properly taken into account.

The differential cross section (eq. A1. 38) is obtained by McCarroll and Salin by evaluating the transition matrix. The transition matrix, T_{if} , is given by either of the two equivalent expressions,¹⁸

$$T_{if} = \langle \phi_f | V_f | \psi_i \rangle \quad (2.20)$$

or

$$T_{if} = \langle \phi_i | V_i | \psi_f \rangle, \quad (2.21)$$

where the subscripts i and f are used to denote initial and final conditions. The first of the two expressions for the transition matrix is evaluated in Appendix 1. Since the single electron charge transfer process is time reversible, the perturbation is given by some appropriate interaction potential between the captured electron and the projectile either before or after the collision indicated by V_i and V_f respectively.

It has already been mentioned that the choice of the static potential in the eikonal phase corresponds to use of the Bates potential, i.e.

$$V_f \approx \frac{Z_b e^2}{x} - \langle \phi_i | \frac{Z_b e^2}{x} | \phi_i \rangle. \quad (2.22)$$

The Bates potential has two desirable features that the BK and JS potentials lack. First, the orthogonality of the wave functions ϕ_i and ϕ_f are maintained. Second, the choice of a zero point energy has no effect on the total or differential cross sections as it should.⁸ However, the Bates calculation is difficult computationally. For this reason, the BK potential is adopted at this point for computational convenience, i.e.

$$V_f = \frac{Z_b e^2}{x}. \quad (2.23)$$

One consequence of using the BK potential is failure of our calculation to produce correctly normalized distributions. It is well known that the BK results generally lie above observed results for total cross sections.⁴

The general form for the eikonal impact parameter method used by Belkic and Salin is presented. Using the BK potential in the evaluation of the probability amplitude (cf. Appendix 2), the differential cross section (eq. A1.38) takes the form,

$$\frac{d\sigma}{d\Omega} = |i\mu v \int_0^\infty \rho d\rho J_0(n\rho) \exp(2i\delta(\rho)) b_{BK}(\rho)|^2, \quad (2.24)$$

where μ is the reduced mass, v is the velocity of the incident projectile, η is the momentum transfer, J_0 is the zero order Bessel function of the first kind, $\delta(\rho)$ is the eikonal phase (eq. 2.19) for the static potential, and $b_{BK}(\rho)$ is the Brinkman-Kramers probability amplitude (eq. A2.30) for the capture of an electron at the impact parameter, ρ . In eq. 2.24, the probability amplitude (eq. A1.37) is separable into the BK probability amplitude times an overall phase (eq. A2.8). The BK probability amplitude given by McGuire and Cocke¹⁹ is

$$b_{BK}(\rho) = \left(\frac{2i n_a}{v} \right) \left(\frac{Z_a Z_b}{n_a n_b} \right)^{5/2} \left(\frac{\rho}{\gamma} \right)^2 K_2 \left(\gamma^{1/2} \rho \right), \quad (2.25)$$

where Z_a and Z_b are the charges of the respective nuclei A and B, n_a and n_b are the principle quantum numbers of the bound electron to the respective nuclei A and B, K_2 is the second order Bessel function of the third kind, and

$$\gamma = \frac{Z_b^2}{n_b^2} + \left(\frac{v}{2} + \frac{1}{2v} \left(\frac{Z_a^2}{n_a^2} - \frac{Z_b^2}{n_b^2} \right) \right)^2. \quad (2.26)$$

Upon specification of the eikonal phase, the integration over impact parameters gives the differential cross section for charge transfer of an electron from the state n_b to state n_a .

CHAPTER 3

APPLICATIONS AND RESULTS

3.1 The Static Brinkman-Kramers Approximation

Use of the static potential (eq. 2.10) in the calculation of the eikonal phase (eq. 2.19) with the BK probability amplitude (eq. 2.25) defines the Static Brinkman-Kramers (SBK) approximation. The static potential for hydrogen and helium like targets is easily evaluated in the independent electron approximation. The form of the eikonal phase using the static potential is now presented.

The average electron-projectile interaction potential (eq. 2.8) using hydrogenic wave functions is readily evaluated for the K shell. The initial wave function²⁰ is

$$\phi_i = \left(\frac{Z^*}{a_0} \right)^{3/2} \frac{1}{2} \exp \left(-\frac{Z^* r}{a_0} \right) \frac{1}{2\sqrt{\pi}} P_0(\cos\theta), \quad (3.1)$$

where Z^* ($Z^* = Z_b$ for a one electron atom) is the effective nuclear charge seen by the bound electrons, and P_0 is the Legendre polynomial. The projectile-electron interaction potential²¹ is

$$-\frac{Z_a}{|\vec{R} - \vec{r}|} = \frac{-Z_a}{r_>} \sum_{l=0}^{\infty} \left(\frac{r_<}{r_>} \right)^l P_l(\cos\theta), \quad (3.2)$$

where R is the internuclear separation distance and r is the electron target separation distance ($r_<$ and $r_>$ refer to the lesser and greater of the two distances). From eq. 3.1 and eq. 3.2, the average projectile - ls electron interaction potential is

$$\bar{V}_e = \frac{-Z}{\pi} \left(\frac{Z^*}{a_0} \right)^3 \int_0^\infty r^2 dr \exp \left(- \frac{2Z^* r}{a_0} \right) \frac{1}{r_>} \\ \times \sum_{\ell=0}^{\infty} \left(\frac{r_<}{r_>} \right)^\ell \int_{-1}^1 P_\ell(\cos\theta) P_0(\cos\theta) P_0(\cos\theta) d(\cos\theta) \int_0^{2\pi} d\phi. \quad (3.3)$$

Upon integration over ϕ and noting that $P_0(\cos\theta) = 1$, eq. 3.3 reads

$$\bar{V}_e = -2Z \left(\frac{Z^*}{a_0} \right)^3 \int_0^\infty r^2 dr \exp \left(- \frac{2Z^* r}{a_0} \right) \frac{1}{r_>} \\ \times \sum_{\ell=0}^{\infty} \left(\frac{r_<}{r_>} \right)^\ell \int_{-1}^1 P_\ell(\cos\theta) P_0(\cos\theta) d(\cos\theta). \quad (3.4)$$

Using the orthogonality of Legendre polynomials,²²

$$\int_{-1}^1 P_\ell(x) P_0(x) dx = 2\delta_{\ell 0}, \quad (3.5)$$

the summation vanished except for the $\ell = 0$ term. This reduces eq. 3.4 to,

$$\bar{V}_e = - \frac{Z}{2} \int_0^\infty \frac{x^2 e^{-x}}{x_>} dx, \quad (3.6)$$

where $x = 2Z^* \frac{r}{a_0}$ and

$$x_> = \begin{cases} R & \text{if } x < \frac{2Z^* R}{a_0} \\ r & \text{if } x > \frac{2Z^* R}{a_0} \end{cases}. \quad (3.7)$$

Since²³

$$\int_t^\infty x e^{-x} dx = e^{-t}(t + 1) \quad (3.8)$$

and

$$\int x^2 e^{-x} dx = e^{-x}(-x^2 - 2x - 2), \quad (3.9)$$

eq. 3.6 is evaluated as

$$\bar{V}_e = -\frac{Z_a}{R} + Z_a \left(\frac{1}{R} + \frac{Z^*}{a_o} \right) \exp \left(-\frac{2Z^* R}{a_o} \right). \quad (3.10)$$

This is precisely the expression that Bassel and Gerjouy⁹(1960) obtained for the average electron interaction for protons on hydrogen ($Z^* = Z_a = 1$). Hence, the static potential (eq. 2.10) for $Z_b \leq 2$ is

$$Z_a Z_b \left(\frac{1}{R} - \frac{1}{R} + \left(\frac{1}{R} + \frac{Z^*}{a_o} \right) \exp \left(-\frac{2Z^* R}{a_o} \right) \right). \quad (3.11)$$

The eikonal phase for the static potential in eq. 3.11 is

$$\delta(\rho) = -\frac{Z_a Z_b}{v} \int_0^\infty \left(\frac{1}{R} + \frac{Z^*}{a_o} \right) \exp \left(-\frac{2Z^* R}{a_o} \right) dz. \quad (3.12)$$

Letting $q = \frac{2Z^*}{a_o}$ and noting $R = \sqrt{\rho^2 + z^2}$, we have

$$\int_0^\infty (\rho^2 + z^2)^{-1/2} \exp(-q(\rho^2 + z^2)^{1/2}) dz \quad (3.13)$$

which is evaluated to be $K_0(\rho q)$ which is the zero-order modified Bessel function of the third kind.²⁴ Since

$$\frac{\partial}{\partial q} \frac{e^{-qR}}{R} = -e^{-qR}, \quad (3.14)$$

we have

$$\int_0^\infty \exp(-q(\rho^2 + z^2)^{1/2}) dz = -\frac{\partial}{\partial q} K_0(\rho q). \quad (3.15)$$

Letting $p = \rho q$, we have²⁵

$$-\rho \frac{\partial}{\partial p} K_0(p) = \rho K_1(p), \quad (3.16)$$

where K_1 is the first order Bessel function of the third kind. The eikonal phase for the static potential is,

$$\delta(\rho) = -\frac{Z_a Z_b}{v} \left[K_0 \left(\frac{2Z^* \rho}{a_o} \right) + \frac{Z^* \rho}{a_o} K_1 \left(\frac{2Z^* \rho}{a_o} \right) \right]. \quad (3.17)$$

Appendix 3 contains a computer program for the calculation of the differential cross section (eq. 2.24) for the static potential in the eikonal phase (eq. 3.17)

3.2 Screened Coulomb Brinkman-Kramers Approximation

For targets with more than two electrons, the static potential contains terms that arise from electrons in shells and subshells other than the K shell. For this reason, there are a multitude of additional terms to be evaluated to obtain the total static potential. To simplify matters, we can approximate the screening of the electrons by the screened Coulomb potential,

$$V(R) = \frac{Z_a Z_b}{R} \exp \left(-\frac{R}{r_o} \right), \quad (3.18)$$

where r_o is an appropriate screening radius. For atom-atom collisions, an expression for the screening radius exists in the literature, given by,^{26,27}

$$r_o = a_o / (Z_a^{2/3} + Z_b^{2/3})^{1/2}. \quad (3.19)$$

Making use of eq. 3.13, the eikonal phase (eq. 2.10) for a screened Coulomb potential (eq. 3.18) is

$$\delta(\rho) = - \frac{Z_a Z_b}{v} \kappa_o \left(\frac{\rho}{r_o} \right). \quad (3.20)$$

Use of the screened Coulomb potential in the eikonal phase with the BK probability amplitude defines the Screened Coulomb Brinkman-Kramers (SCBK) approximation.

The limiting cases for screening give the results of Brinkman and Kramers and the results of Belkic and Salin. When the screening radius is zero the screened Coulomb potential vanishes, i.e.

$$\frac{Z_a Z_b}{R} \exp \left(- \frac{R}{r_o} \right) \xrightarrow{r_o \rightarrow 0} 0. \quad (3.21)$$

This corresponds to the calculation of Brinkman and Kramers. When the screening radius is infinite the screened Coulomb potential reduces to the Coulomb potential, i.e.

$$\frac{Z_a Z_b}{R} \exp \left(- \frac{R}{r_o} \right) \xrightarrow{r_o \rightarrow \infty} \frac{Z_a Z_b}{R}. \quad (3.22)$$

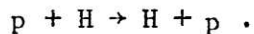
This is the potential used by Belkic and Salin to obtain the Coulomb Brinkman-Kramers (CBK) approximation.

Appendix 4 contains a program for the calculation of the differential cross section (eq. 2.24) using the screened Coulomb potential in the eikonal phase (eq. 3.20).

3.3 Protons on Hydrogen

We can now test the effects of screening of the internuclear poten-

tial by the target electrons in the charge transfer process. Consider the simplest possible system of a proton incident upon atomic hydrogen, i.e.

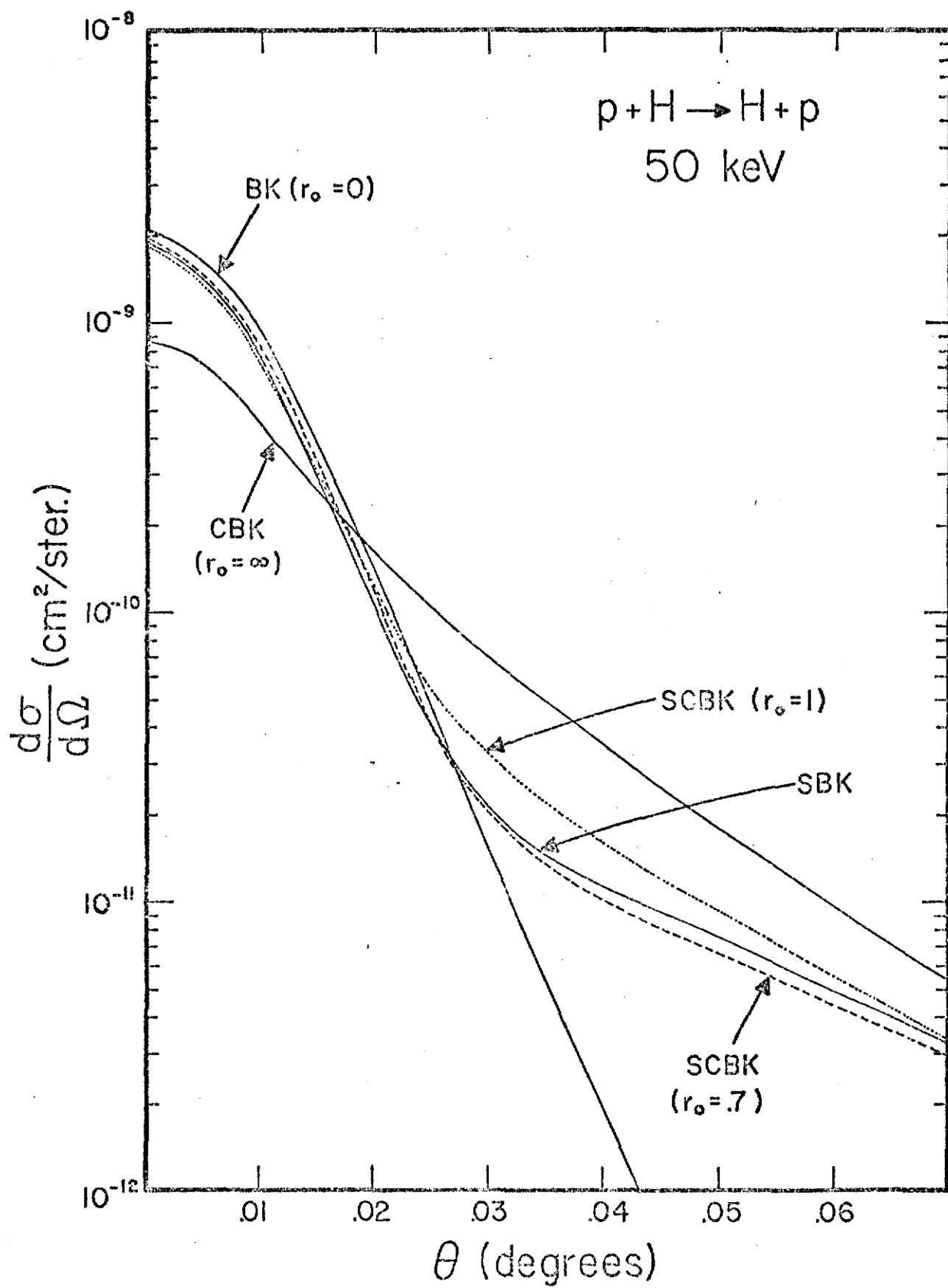


In viewing this reaction, we compare the differential cross section of SCBK, for several screening radii, with SBK.

There are several interesting features of SCBK and SBK. In figure 3, a comparison of the differential cross sections versus angle is presented for protons incident upon atomic hydrogen at 50 keV. There are three distinct curve shapes (solid lines). The screened Coulomb Brinkman-Kramers calculation reduces to the Brinkman-Kramers calculation and the Coulomb Brinkman-Kramers calculation of Belkic and Salin in the limiting cases of screening parameters. The total cross sections from all the differential cross sections in figure 3 are identical. Finally, the shape of SCBK is not sensitive to reasonable choices of the screening parameter.

There are three distinct shapes for the differential cross section indicated by the solid curves in figure 3. The BK angular distribution is peaked in the forward direction and falls off rapidly at the larger angles, for the BK calculation takes into account no internuclear interaction. On the other hand, the CBK calculation takes into account the full internuclear interaction i.e. $V(R) = \frac{1}{R}$, where R is the internuclear separation distance. As a result, the curve marked CBK shows that the capture process at the larger angles is orders of magnitude above the BK results due to inclusion of the internuclear repulsion within the eikonal phase. Recalling the discussion of figure 2, the SBK calculation gives the desired results of following BK at the forward angles ($\theta < \frac{m_e}{m_p}$) and CBK at large

Figure 3. The differential cross section for electron capture by 50 keV protons incident on atomic hydrogen is shown. The curve marked BK is the Brinkman-Kramers approximation, CBK is the Coulomb Brinkman-Kramers approximation, SBK is the Static Brinkman-Kramers approximation, and SCBK the Screened Coulomb Brinkman-Kramers approximation.



angles ($\theta > \frac{m_e}{m_p}$, where m_e is the mass of the electron and m_p is the projectile mass). The charge parameters used are $Z_a = Z_b = Z^* = 1$.

The SCBK calculation reduces to BK and CBK in the limiting cases for screening parameters. The BK curve in figure 3 is obtained by choosing the screening radius in SCBK to be 10^{-2} , cf. eq. 3.21. The CBK curve is obtained by choosing the screening radius in SCBK to be 10^2 , cf. eq. 3.22. There were difficulties in choosing extreme values for the screening parameter due to the Bessel function subroutines. However, it is noted that in atomic dimensions $10^{-2} \approx 0$ and $10^2 \approx \infty$. This serves as a check on the SCBK program.

The total integrated cross sections for BK, CBK, and SBK are identical. This is because the eikonal phase appears as an overall phase in the probability amplitude (eq. A2.8), i.e.

$$\begin{aligned}\sigma_{\text{Total}} &= 2\pi \int |b(\rho)|^2 \rho d\rho \\ &= 2\pi \int |b_{\text{BK}}(\rho)|^2 \rho d\rho \\ &= \sigma_{\text{BK}},\end{aligned}\tag{3.23}$$

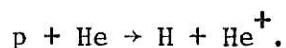
where $b(\rho)$ is the probability amplitude (eq. A2.8), $b_{\text{BK}}(\rho)$ is the BK probability amplitude (eq. 2.9), ρ is the impact parameter, σ_{Total} is the total cross section, and σ_{BK} is the BK total cross section. The total integrated cross sections BK, SBK, and CBK are in agreement with the closed form expression for the total BK cross section of $2.96 \cdot 10^{-16} \text{ cm}^2$. This serves as a check on the various integration techniques used in the SBK and SCBK computer programs.

The shape of SCBK is not sensitive to reasonable choices of the

screening parameter. That is, the SCBK calculation for screening radii on the order the K shell radius (dotted and dashed curves in figure 3) retains the two region shape of the SBK calculation. For the Bohr screening radius (eq. 3.19), the SCBK calculation (dashed line) closely follows that of SBK. This indicates that the screened Coulomb potential with Bohr screening is a good approximation to the static potential.

3.4 Protons on Helium

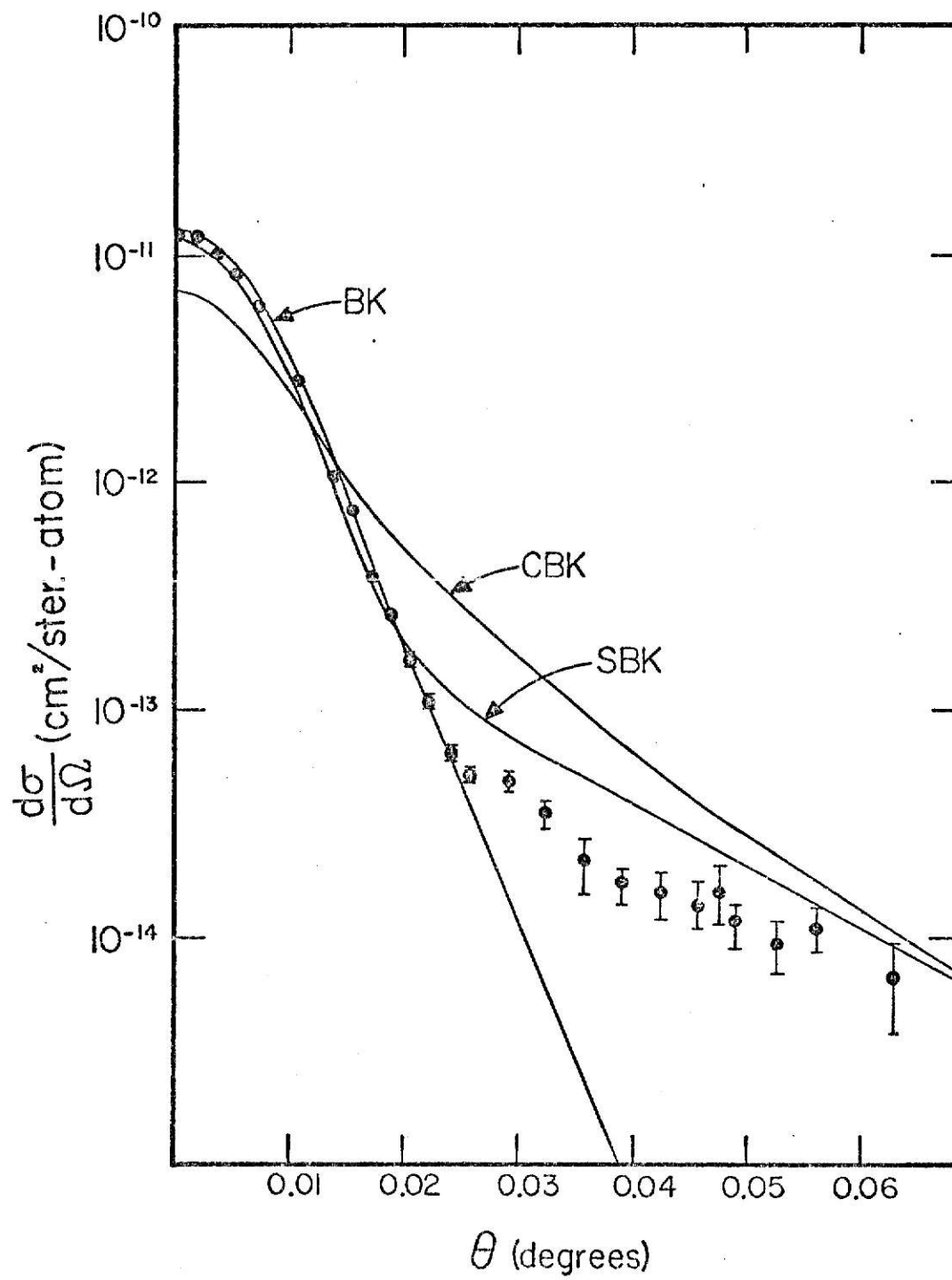
Although the angular distribution for protons incident on atomic hydrogen is easiest to treat theoretically, it is difficult to measure experimentally simply because hydrogen is diatomic. A comparison with observed differential cross sections is necessary to check the screening effects of the electrons on the internuclear potential in the SBK approximation. For these reasons we choose to consider the charge transfer process,



Data for this reaction exists at 293 keV observed by Bratton,²⁸ et al., (1977).

The differential cross section for 293 keV protons incident on helium is compared with the normalized theoretical predictions of BK, CBK, and SBK (cf. figure 4). The fact that the theoretical predictions must be reduced by a factor of 3.55 to agree with the observed cross section of $9.4 \cdot 10^{-19} \text{ cm}^2/\text{atom}$ indicates a poor assumption has been made. The charge parameters used in the SBK calculation are $Z_a = 1$, $Z_b = 2$ and $Z^* = 1.618$. We believe the weakest assumption made is use of the BK probability amplitude in our calculation, for it is well known that the BK results generally lie above the observed total cross sections. Nevertheless, we are testing

Figure 4. Differential cross section in laboratory system for capture of K-shell electrons from helium by 293 keV protons. The curve marked BK represents the normalized Brinkman-Kramers approximation; CBK, the normalized Coulomb Brinkman-Kramers approximation, and SBK, the normalized Static Brinkman-Kramers approximation. Each theoretical curve has been reduced by a factor of 3.55 normalizing total cross sections to observed results of $9.4 \cdot 10^{-19} \text{ cm}^2/\text{atom}$. Experimental data are those of Bratton, et al., (1977).

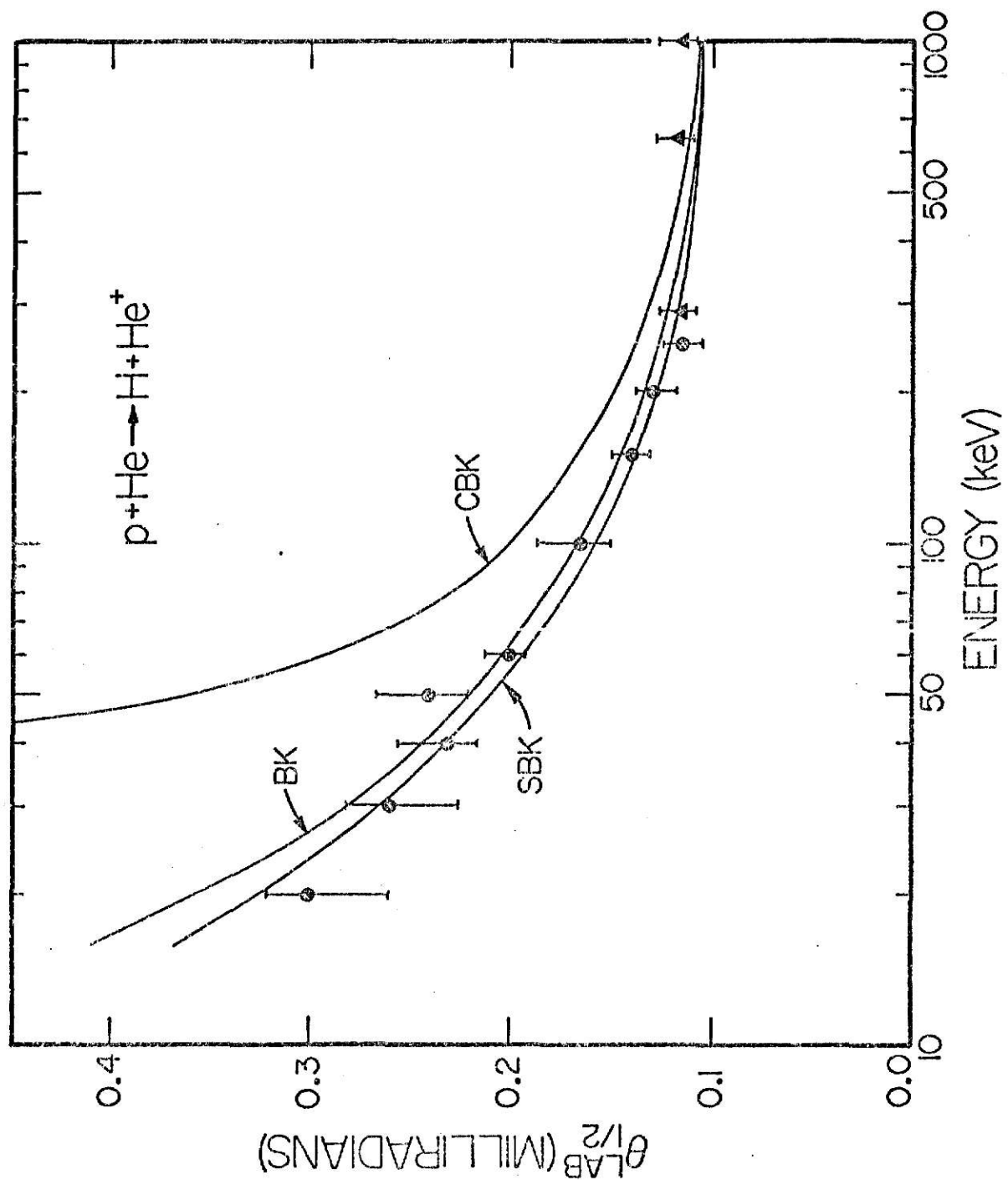


the screening effects on the differential cross section and not the BK approximation. Hence, when comparing our predictions with data, normalization is unavoidable when the BK probability amplitude is used.

There is evidence that a normalization factor is justified for bringing the SBK approximation into close agreement with observation. A recent close coupling calculation of the Bates probability amplitude by Lin¹⁰ indicates the Bates probability amplitude exhibits the same impact parameter dependence as the BK probability amplitude times a constant factor. In addition, the total cross section from this calculation is in agreement with that observed by Bratton, et al., (1977). Another justification of the normalization of SBK is witnessed in a plot of the laboratory angle $\theta_{1/2}$ where the scattering distribution falls to half the maximum intensity as a function of the projectile energy,²⁹ cf. figure 5. A normalization factor is not an issue in the calculation of $\theta_{1/2}$ since we are considering a ratio of intensities.

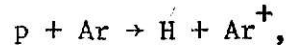
SBK gives a better fit to the data than CBK or BK. Referring to figure 4, it is seen that the SBK calculation features two regions, the forward angle region where BK gives a reasonable fit to the data and the large angle region where CBK gives reasonable fit to the data. Referring to figure 5, it is seen that the SBK approximation is superior to CBK in its agreement with data. This is because CBK follows the angular distribution at large angles whereas $\theta_{1/2}$ is calculated at the forward angle region where CBK is in poor agreement. A similar argument can be given as to why BK and SBK agree in the calculation of $\theta_{1/2}$. However, it should be noted that the BK approximation does not give good agreement for large angle capture as witnessed in the angular distribution in figure 4.

Figure 5. The laboratory angle $\theta_{1/2}$ where the scattering distribution falls to half the maximum intensity as a function of the projectile energy. The curve marked BK represents results using the Brinkman-Kramers approximation; SBK using the Static Brinkman-Kramers approximation; and CBK the Coulomb Brinkman-Kramers approximation. Experimental data are due to (o) Wittkower and Gilbody³⁰(1967), and (Δ) Bratton,³¹ (1977).



3.5 Protons on Argon

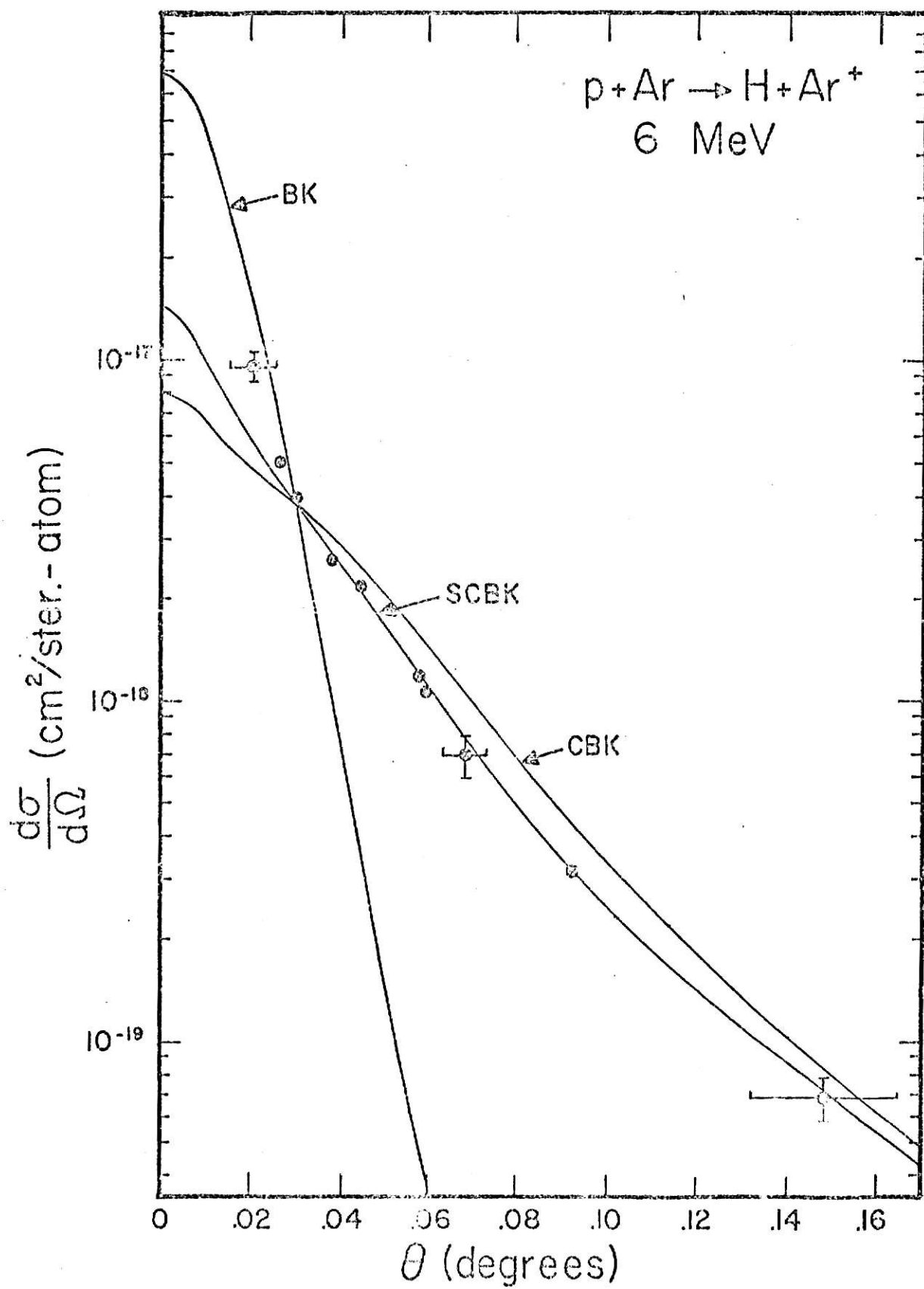
In considering the reaction of protons incident on helium, a normalization factor was introduced to bring the BK, CBK, and SBK calculations into agreement with the experimental total cross section. For the reaction



the BK total cross section is in close agreement with the data at a projectile energy of 6 MeV. For this reaction, we compare the SCBK approximation to the data without normalization.

Using hydrogenic wave functions as before and charge parameters $Z_a = 1$ and $Z_b = Z^* = 18$, we calculate BK, CBK and SCBK, cf. figure 6. These are precisely the results obtained by Belkic and Salin for the BK and CBK approximations in figure 2. The SCBK results are obtained for Bohr screening which corresponds to the SBK approximation. The total cross section for BK (i.e. all curves) is $1.78 \cdot 10^{-23} \text{ cm}^2/\text{atom}$ which compares with the experimental results³² of $(1.68 \pm 0.9) \times 10^{-23} \text{ cm}^2/\text{atom}$. Again the screened Coulomb Brinkman-Kramers approximation is in better agreement with the data than either BK or CBK at both the large and small angles.

Figure 6. Differential cross section in laboratory system for the capture of K-shell electrons from argon by 6 MeV protons. The curve marked BK is the Brinkman-Kramers approximation; CBK, the Coulomb Brinkman-Kramers approximation, and SCBK the Screened Coulomb Brinkman-Kramers approximation. Experimental data are those of Cocke, et al., (1976).



CHAPTER 4

CONCLUSION

The role of the internuclear potential in angular distributions has been examined. Using the eikonal method of McCarroll and Salin, the effective internuclear potential is represented by the static potential. The shape of the angular distribution using this static potential gives improved agreement with observed results of Bratton, et al., over that obtained by Belkic and Salin using an unscreened Coulomb potential and much better agreement than Brinkman and Kramers which takes into account no internuclear repulsion.

As a consequence of choosing the static potential to represent the effective internuclear potential, the electron capture potential is found to be the potential prescribed by Bates. Although the Brinkman-Kramers potential is used to approximate the Bates electron capture potential, the shape of the differential cross section in the Static Brinkman-Kramers (SBK) approximation exhibits two distinct regions in the differential cross section corresponding to observation by Bratton, et al. In contrast to other methods, the SBK approximation has no node in the differential cross section. Since the static potential and the Bates potential are intimately related, the SBK results reinforce use of the Bates potential.

However, our SBK approximation suffers from various limitations. Possible improvements in our calculation include:

- i) use of the Bates potential in calculating the electron capture probability amplitude,
- ii) use of better wave functions to describe the bound electron, and

iii) taking into account second order effects.

Other effects are probably less important than these although they may contribute to a total understanding of charge transfer.

REFERENCES

1. R. Shakeshaft, J. Phys. B 7, 1059 (1974).
2. H. C. Brinkman and H. A. Kramers, Proc. Acad. Sci. Amst. 33, 973 (1930).
3. J. R. Oppenheimer, Phys. Rev. 31, 349 (1928).
4. V. S. Nikolaev, Zh. Eksp. Teor. Fiz. 51, 1263 (1966), Sov. Phys. JETP 24, 847 (1967).
5. J. D. Jackson and H. Schiff, Phys. Rev. 89, 359 (1953).
6. R. A. Mapleton, J. Phys. B 1, 529 (1968).
7. A. M. Halpern and J. Law, Bull. Am. Phys. Soc. 19, 561 (1974); Phys. Rev. A 12, 1776 (1975).
8. D. R. Bates, Proc. Roy. Soc. (London) A247, 294 (1958).
9. R. H. Bassel and E. Gerjuoy, Phys. Rev. 117, 749 (1960).
10. C. D. Lin, S. C. Soong, and L. Tunnell, private communication (1977).
11. Dz. Belkic and A. Salin, J. Phys. B 9, L397 (1976).
12. C. L. Cocke, J. R. Macdonald, B. Curnutte, S. L. Varghese, and P. Randall, Phys. Rev. Lett. 36, 782 (1976).
13. L. I. Schiff, Quantum Mechanics (McGraw-Hill, New York, 1968) 3rd ed., pp. 314-315. Eq. 2.3-2.5 are presented in Schiff as well as other texts.
14. J. H. McGuire and L. Weaver, Phys. Rev. A 16, to be published (1977).
15. J. R. Taylor, Scattering Theory: The Quantum Theory on Nonrelativistic Collisions (Wiley and Sons, New York, 1972), p. 153.
16. Reference 13, pp. 339-341.
17. R. McCarroll and A. Salin, J. Phys. B 1, 163 (1968).
18. M. R. C. McDowell and J. P. Coleman, Introduction to the Theory of Ion-Atom Collisions (American Elsevier Publishing Company, New York, 1970), p. 279.

19. L. H. McGuire and C. L. Cocke, "BK Probabilities for Electron Capture", Kansas State University, unpublished (1977).
20. A. Messiah, Quantum Mechanics (Wiley and Sons, New York, 1958) Vol. I, p. 484.
21. Reference 20, p. 497.
22. Reference 20, p. 493.
23. S. M. Selby, Standard Mathematical Tables (CRC Press, Cleveland, 1973) 23rd ed., p. 453.
24. I. S. Gradshteyn and I. M. Ryzhik, Table of Integrals, Series, and Products (Academic Press, New York, 1965), p. 959.
25. Reference 24, p. 970.
26. N. Bohr, Kgl. Danske Videnskab. Selskab, Mat-fys. Medd. 18, 8 (1948).
27. E. Everhart, G. Stone, and R. J. Carbone, Phys. Rev. 99, 1287 (1955).
28. T. Bratton, C. L. Cocke, and J. R. Macdonald, J. Phys. B, (to be published).
29. S. R. Rogers and J. H. McGuire, J. Phys. B, (to be published).
30. A. B. Wittkower and H. B. Gilbody, Proc. Phys. Soc. 90, 343 (1967).
31. T. R. Bratton, Master's Thesis Kansas State University (1977), (unpublished).
32. J. R. Macdonald, C. L. Cocke, and W. W. Eidson, Phys. Rev. Lett. 32, 648 (1974).
33. H. Schiff, Can. J. Phys. 32, 393 (1954).
34. R. J. Glauber, Lectures in Theoretical Physics (Interscience, New York, 1958) Vol. 1, pp. 315-424.
35. M. Abramowitz and I. A. Stegun, Handbook of Mathematical Functions with Formulas, Graphs, and Mathematical Tables (Dover Publications, New York, 1972), p. 360.
36. Reference 18, pp. 212-215.

APPENDIX 1

The Transition Matrix

The form of the transition matrix developed in this section closely follows that outlined by McCarroll and Salin (1968). Related results have previously been given by Schiff³³(1954) and Glauber³⁴(1958). From this development the validity of the expressions for the transition matrix, and hence the differential cross section, is clearly shown.

Consider the charge transfer process,



A diagram of the position vectors for this reaction is given in Figure 7. This diagram is used extensively in the steps to follow. In addition, some vector relations corresponding to the diagram are used:

$$\vec{x} = \vec{r}_2 - \vec{r}_1 \quad (\text{A1.1})$$

$$\vec{s} = \vec{r}_2 - \vec{r}_3 \quad (\text{A1.2})$$

$$\vec{R} = \vec{r}_3 - \vec{r}_1 = \vec{x} - \vec{s} \quad (\text{A1.3})$$

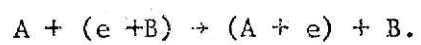
$$\vec{r} = \frac{1}{2} (\vec{x} + \vec{s}). \quad (\text{A1.4})$$

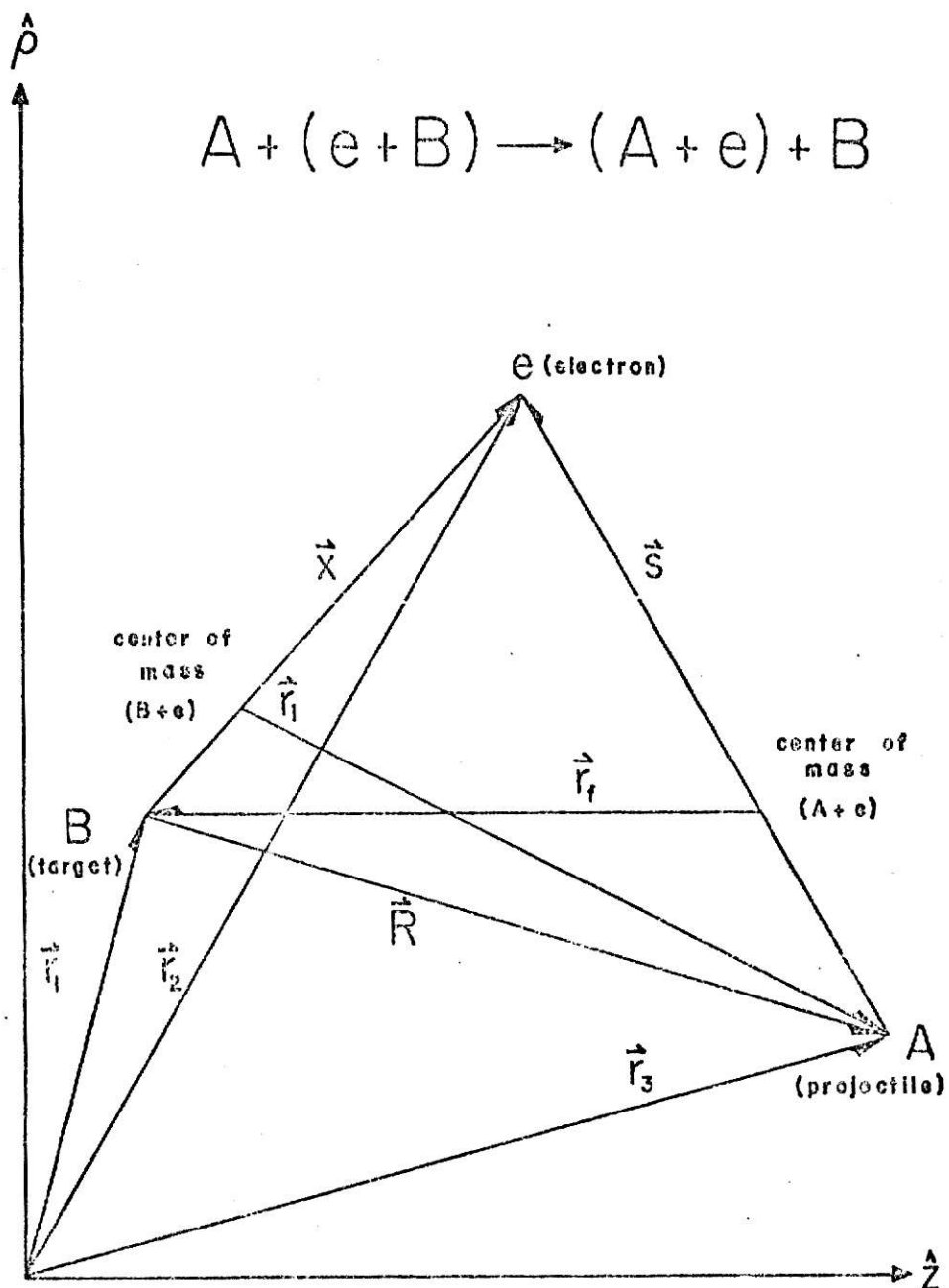
Letting m_a be the mass of the projectile and m_b be the mass of the target, the following vector quantities are defined from the reduced mass relations for the respective electron-nucleus systems:

$$\vec{r}_1 + \vec{s} = \frac{m_b}{m_b + 1} \vec{x} \quad (\text{A1.5})$$

and

Figure 7. The coordinates for the charge transfer process





$$\vec{r}_f + \vec{x} = \frac{m_a}{m_a + 1} \vec{s}. \quad (\text{A1.6})$$

Upon substitution for \vec{x} and \vec{s} (eq. A1.1 and eq. A1.2) eq. A1.5 and A1.6 become,

$$\vec{r}_i = \vec{r}_3 - \frac{m_b \vec{r}_1 + \vec{r}_2}{m_b + 1} \quad (\text{A1.7})$$

$$\vec{r}_f = \vec{r}_1 - \frac{m_a \vec{r}_3 + \vec{r}_2}{m_a + 1}. \quad (\text{A1.8})$$

A two state wave expansion of the total wave function within the independent electron model is

$$\Psi = \phi_b(\vec{x})F(\vec{r}_i) + \phi_a(\vec{s})G(\vec{r}_f), \quad (\text{A1.9})$$

where $\phi_a(\vec{s})$ and $\phi_b(\vec{x})$ are the bound state functions of the active electron around nuclei A and B, respectively. The asymptotic conditions on Ψ are

$$F(\vec{r}_i) \xrightarrow[\vec{r}_i \rightarrow \infty]{} \exp(i\vec{k}_i \cdot \vec{r}_i) + O\left(\frac{1}{r_i}\right)$$

and

$$G(\vec{r}_f) \xrightarrow[\vec{r}_f \rightarrow \infty]{} O\left(\frac{1}{r_f}\right). \quad (\text{A1.11})$$

The scattered waves are shown to fall off as $\exp(ikr)/r$, i.e. $O(\frac{1}{r})$.

It is now of relative importance to introduce the quantities,

$$F(\vec{r}_i) \equiv \exp(-i\vec{k}_i \cdot \vec{r}_i)F(\vec{r}_i) \quad (\text{A1.12})$$

and

$$G(\vec{r}_f) \equiv \exp(i\vec{k}_i \cdot \vec{r}_f) G(\vec{r}_f). \quad (A1.13)$$

This phase transformation is made for later simplification in the transition matrix.

The transition matrix (eq. 2.18) is now given by,

$$\begin{aligned} T_{if} &\equiv \langle \phi_f | V_f | \psi_i \rangle \\ &= \langle \phi_a(\vec{s}) \exp(-i\vec{k}_f \cdot \vec{r}_f) | V_f | \psi_i \rangle, \end{aligned} \quad (A1.14)$$

where ψ is given by eq. A1.9. Substitution of $F(\vec{r}_i)$ and $G(\vec{r}_f)$ from eqs. A1.12 and A1.13 gives,

$$\psi = \exp(i\vec{k}_i \cdot \vec{r}_i) L(\vec{x}, \vec{r}_i), \quad (A1.15)$$

where

$$L(\vec{x}, \vec{r}_i) = \phi_b(\vec{x}) F(\vec{r}_i) + \phi_b(\vec{s}) G(\vec{r}_f) \exp\left[-i\vec{k}_i \cdot (\vec{r}_f + \vec{r}_i)\right]. \quad (A1.16)$$

It then follows that the transition matrix is given by,

$$T_{if} = \int d\vec{R} \int d\vec{r} \phi_a^*(\vec{s}) \exp\left[i(\vec{k}_f \cdot \vec{r}_f + \vec{k}_i \cdot \vec{r}_i)\right] V_f L(\vec{x}, \vec{r}_i) \quad (A1.17)$$

Modification of the exponential phase in eq. A1.17 is needed. Consider,

$$\begin{aligned} \vec{k}_f \cdot \vec{r}_f + \vec{k}_i \cdot \vec{r}_i &= \vec{k}_i \cdot \vec{r}_f - \vec{k}_i \cdot \vec{r}_f + \vec{k}_f \cdot \vec{r}_f + \vec{k}_i \cdot \vec{r}_i \\ &= (\vec{k}_f - \vec{k}_i) \cdot \vec{r}_f + \vec{k}_i \cdot (\vec{r}_i + \vec{r}_f) \end{aligned} \quad (A1.18)$$

$$= -\vec{\eta} \cdot \vec{r}_f + \vec{k}_i \cdot (\vec{r}_i + \vec{r}_f), \quad (A1.19)$$

where the definition,

$$\vec{\eta} \equiv \vec{k}_i - \vec{k}_f, \quad (\text{A1.20})$$

is used. Utilizing eq. A1.3 and eq. A1.6 (also see diagram) it follows

$$-\vec{r}_f \approx \vec{R}, \quad (\text{A1.21})$$

since $m_a \gg 1$. Combining eq. A1.19 and eq. A1.21, the phase is

$$\vec{k}_f \cdot \vec{r}_f + \vec{k}_i \cdot \vec{r}_i \approx \vec{\eta} \cdot \vec{R} + \vec{k}_i \cdot (\vec{r}_i + \vec{r}_f). \quad (\text{A1.22})$$

Noting that

$$\vec{R} = z\hat{z} + \vec{\rho}, \quad (\text{A1.23})$$

where \hat{z} is chosen to be $(2k_i)^{-1}(\vec{k}_i + \vec{k}_f)$ and $\vec{\rho}$ is the plane of impact parameters perpendicular to \hat{z} , eq. A1.22 becomes

$$\vec{k}_f \cdot \vec{r}_f + \vec{k}_i \cdot \vec{r}_i \approx \vec{\eta} \cdot \vec{z} + \vec{\eta} \cdot \vec{\rho} + \vec{k}_i \cdot (\vec{r}_i + \vec{r}_f). \quad (\text{A1.24})$$

However, it is observed

$$\vec{\eta} \cdot \vec{z} = \frac{k_i^2 - k_f^2}{2k_i} z. \quad (\text{A1.25})$$

From conservation of energy, we have

$$\frac{k_i^2}{2\mu_i} + \epsilon_i = \frac{k_f^2}{2\mu_f} + \epsilon_f, \quad (\text{A1.26})$$

where ϵ_i and ϵ_f are the initial and final binding energies of the electrons to the respective nuclei B and A. Combining eq. A1.25 with eq.

A1.26 and noting that

$$\mu \equiv \mu_i = \frac{(m_b + 1)m_a}{m_a + m_b + 1} \approx \frac{(m_a + 1)m_b}{m_a + m_b + 1} = \mu_f, \quad (\text{A1.27})$$

we get

$$\vec{\eta} \cdot \vec{z} = -\frac{\epsilon_f - \epsilon_i}{v} z, \quad (\text{A1.28})$$

where $\mu v = k_i$ is used. Defining $\Delta E \equiv \epsilon_f - \epsilon_i$ and substituting eq. A1.28 into eq. A1.24, the phase takes the form

$$\vec{k}_f \cdot \vec{r}_f + \vec{k}_i \cdot \vec{r}_i \approx \vec{\eta} \cdot \vec{\rho} + \vec{k}_i \cdot (\vec{r}_i \cdot \vec{r}_f) + \frac{\Delta E}{v} z. \quad (\text{A1.29})$$

Replacing the phase in the transition matrix (eq. A1.17) by eq. A1.29, we obtain

$$T_{if} \approx \int \exp(i\vec{\eta} \cdot \vec{\rho}) d\vec{\rho} \int_{-\infty}^{\infty} dz \int d\vec{r}_a \phi_a^*(\vec{s}) \exp(i\xi) V_f L(\vec{x}, \vec{r}_i), \quad (\text{A1.30})$$

where

$$\xi \equiv \vec{k}_i \cdot (\vec{r}_i + \vec{r}_f) + \frac{\Delta E}{v} z. \quad (\text{A1.31})$$

Considering only s state to s state electron capture gives our system cylindrical symmetry. Hence, the integration over the plane of impact parameters becomes

$$d\vec{\rho} = \rho d\rho d\alpha \quad (\text{A1.32})$$

and

$$\vec{\eta} \cdot \vec{\rho} = \eta \rho \cos \alpha, \quad (\text{A1.33})$$

where α is the azimuthal angle. The integral,

$$\int_0^{2\pi} \exp(in\rho \cos\alpha) d\alpha \quad (\text{A1.34})$$

is evaluated³⁵ to be,

$$2\pi J_0(\eta\rho), \quad (\text{A1.35})$$

where J_0 is the zero order Bessel function of the first kind. Using the result of eq. A1.35, the transition matrix (eq. A1.30) becomes

$$T_{if} \approx -i2\pi v \int_0^\infty \rho d\rho J_0(\eta\rho) b(\rho), \quad (\text{A1.36})$$

where

$$b(\rho) = \frac{i}{v} \int_{-\infty}^{\infty} dz \int d\vec{r}_a {}^*(\vec{s}) \exp(i\xi) V_f L(\vec{x}, \vec{r}_i). \quad (\text{A1.37})$$

It follows immediately (eq. A1.36 and eq. 2.6) that the differential cross section is given by,

$$\frac{d\sigma}{d\Omega} \approx |-i\mu v \int_0^\infty \rho d\rho J_0(\eta\rho) b(\rho)|^2. \quad (\text{A1.38})$$

In arriving at eq. A1.38 near elastic scattering, i.e. $k \equiv k_i \approx k_f$, is assumed.

APPENDIX 2

The Brinkman Kramers Probability Amplitude

The probability that a projectile will capture an electron at a given impact parameter, ρ , is

$$\text{Probability} = |b(\rho)|^2, \quad (\text{A2.1})$$

where $b(\rho)$ is the probability amplitude. From appendix 1, the probability amplitude is given by

$$b(\rho) = \frac{-i}{v} \exp(2i\delta(\rho)) \int_{-\infty}^{\infty} dz \int d\vec{r} \phi_a^*(\vec{s}) \exp(i\xi) \frac{z_b}{x} \phi_b(\vec{x}), \quad (\text{A2.2})$$

where the BK potential (eq. 2.23) and the projectile wave function (eq. 2.18) are used. Note in the eikonal phase, we have $\vec{k}_i \parallel \hat{z}$. In the probability amplitude (eq. A1.37), we have $\vec{k}_i + \vec{k}_f \parallel \hat{z}$. For small angle scattering, \vec{k}_i is approximately parallel to $\vec{k}_i + \vec{k}_f$.

Using the definitions of the reduced mass (eq. A1.27) and the vector relations (eq. A1.3 - eq. A1.6), the phase (eq. A1.31) becomes

$$\xi = (f + g)\vec{v} \cdot \vec{r} + \frac{1}{2}(g - f)\vec{v} \cdot \vec{R} + \frac{\Delta E}{v} z, \quad (\text{A2.3})$$

where

$$f \equiv - \frac{m_a}{(m_a + 1)} \frac{(m_b + 1)}{(m_a + m_b + 1)} \quad (\text{A2.4})$$

and

$$g \equiv - \frac{m_a}{m_a + m_b + 1}. \quad (\text{A2.5})$$

Noting that

$$\mathbf{v}_z \hat{\mathbf{z}} \approx \vec{\mathbf{v}} \quad (\text{A2.6})$$

and that within $O(\frac{1}{\mu})$

$$f + g \approx -1, \quad (\text{A2.7})$$

the probability amplitude (eq. A2.2) becomes

$$b(\rho) = -b_{BK}(\rho) \exp(2i\delta(\rho)), \quad (\text{A2.8})$$

where

$$b_{BK}(\rho) = \frac{i}{v} \int_{-\infty}^{\infty} dz \exp(i(\frac{v}{2}(g - f)z + \frac{\Delta E}{v}z)) \\ \times \int d\vec{r} \phi_a^*(\vec{s}) \frac{Z_b}{x} \phi_b(\vec{x}) \exp(-i\vec{v} \cdot \vec{r}) \quad (\text{A2.9})$$

Following the Fourier transform method of McDowell and Coleman,³⁶ the probability amplitude for symmetric charge capture ($Z_a = Z_b \equiv Z$ and $m_a = m_b \equiv M$) is

$$b_{BK}(\rho) = \frac{i}{v} \int_{-\infty}^{\infty} dz \exp(i\frac{\Delta E}{v}z) \int d\vec{r} \phi_a^*(\vec{s}) \frac{Z_b}{x} \phi_b(\vec{x}) \exp(-i\vec{v} \cdot \vec{r}). \quad (\text{A2.10})$$

By performing the Fourier transforms on

$$f_a(\vec{k}) \equiv \int \phi_a(\vec{s}) \exp(-i\vec{k} \cdot \vec{s}) d\vec{s} \quad (\text{A2.11})$$

and

$$g_b(\vec{k}) \equiv \int \phi_b(\vec{x}) \frac{Z_b}{x} \exp(-i\vec{k} \cdot \vec{x}) d\vec{x} \quad (\text{A2.12})$$

to give

$$\phi_a(\vec{s}) = (2\pi)^{-3} \int f_a(\vec{k}) \exp(i\vec{k} \cdot \vec{s}) d\vec{k} \quad (A2.13)$$

and

$$\frac{z_b}{x} \phi_b(\vec{x}) = (2\pi)^{-3} \int g_b(\vec{k}) \exp(i\vec{k} \cdot \vec{x}) d\vec{k}, \quad (A2.14)$$

eq. A2.10 is

$$\begin{aligned} b_{BK}(\rho) &= \frac{1}{v} (2\pi)^{-6} \int_{-\infty}^{\infty} dz \exp(i \frac{\Delta E}{v} z) \int d\vec{k} \int d\vec{k}' f_a(\vec{k})^* g_b(\vec{k}') \\ &\times \int d\vec{r} \exp(i(\vec{k}' \cdot \vec{x} - \vec{k} \cdot \vec{s} - \vec{v} \cdot \vec{r})). \end{aligned} \quad (A2.15)$$

From eq. A1.3 and eq. A1.4,

$$\vec{x} = \vec{r} + \frac{1}{2} \vec{R} \quad (A2.16)$$

and

$$\vec{s} = \vec{r} - \frac{1}{2} \vec{R}, \quad (A2.17)$$

the integration over \vec{r} reduces eq. A2.15 to

$$\begin{aligned} b_{BK}(\rho) &= \frac{1}{v} (2\pi)^{-3} \int_{-\infty}^{\infty} dz \exp(i \frac{\Delta E}{v} z) \exp(i \frac{1}{2} \vec{v} \cdot \vec{R}) \\ &\times \int d\vec{k} f_a(\vec{k})^* g_b(\vec{k} + \vec{v}) \exp(i\vec{k} \cdot \vec{R}). \end{aligned} \quad (A2.18)$$

Recalling that

$$\vec{R} = \rho \hat{\rho} + z \hat{z} \quad (A2.19)$$

and choosing

$$\vec{k} = k_x \hat{x} + k_y \hat{y} + k_z \hat{z} \quad (A2.20)$$

such that $\hat{x}||\hat{\rho}$, the BK probability amplitude (eq. A2.18) is

$$b_{BK}(\rho) = \frac{1}{v} (2\pi)^{-3} \int_{-\infty}^{\infty} dk_x \int_{-\infty}^{\infty} dk_y \int_{-\infty}^{\infty} dk_z f_a(k_x, k_y, k_z)^* \times g_b(k_x, k_y, k_z + v) \exp(i\rho k_x) \int_{-\infty}^{\infty} dz \exp(iz(\frac{v}{2} + k_z)). \quad (A2.21)$$

At this time, we further limit our development of the BK probability amplitude to consider K shell to K shell capture. The 1s wave function in momentum space is

$$f_a(k) = \frac{8\pi^{\frac{1}{2}} Z_a^{5/2}}{(k^2 + Z_a^2)^2} \quad (A2.22)$$

which gives

$$g_b(\vec{k} + \vec{v}) = \frac{4\pi^{\frac{1}{2}} Z_b^{5/2}}{((\vec{k} + \vec{v})^2 + Z_b^2)}. \quad (A2.23)$$

Completing the integration over \vec{z} and substituting eq. A2.22 and eq. A2.23, eq. A2.21 is

$$b_{BK}(\rho) = \frac{i8Z^5}{\pi v} \int_{-\infty}^{\infty} dk_x \int_{-\infty}^{\infty} dk_y \exp(i\rho k_x) (k_x^2 + k_y^2 + \beta)^{-3}, \quad (A2.24)$$

where

$$\beta = \frac{v^2}{4} + Z^2. \quad (A2.25)$$

Integrating over k_y , eq. A2.24 reduces to

$$b_{BK}(\rho) = \frac{i6Z^5}{v} \int_0^{\infty} \frac{\cos(\rho k_x)}{(k_x^2 + \beta)^{5/2}} dk_x. \quad (A2.26)$$

The last integration, eq. A2.26 is

$$b_{BK}(\rho) = \left(\frac{2i}{v} \right) Z^5 \left(\frac{\rho^2}{\beta} \right) K_2 \left(\beta^{\frac{1}{2}} \rho \right), \quad (A2.27)$$

where K_2 is the second-order modified Bessel function of the third kind. This corresponds to the transition probability amplitude calculated in a straight-line impact parameter method given by Belkic and Salin as,

$$b_{BK}(\rho) = \left(\frac{2i}{v} \right) (Z_a Z_b)^{5/2} \left(\frac{\rho^2}{\gamma_o} \right) K_2 \left(\gamma_o^{\frac{1}{2}} \rho \right), \quad (A2.28)$$

where

$$\gamma_o = Z_b^2 + \left(\frac{v}{2} + \frac{\Delta E}{v} \right)^2. \quad (A2.29)$$

An even more general expression given by McGuire and Cocke is given as,

$$b_{BK}(\rho) = \left(\frac{2in_a}{v} \right) \left(\frac{Z_a Z_b}{n_a n_b} \right)^{5/2} \left(\frac{\rho^2}{\gamma} \right) K_2 \left(\gamma^{\frac{1}{2}} \rho \right), \quad (A2.30)$$

where

$$\gamma = \frac{Z_b^2}{n_b^2} + \left(\frac{v}{2} + \frac{1}{2v} \left(\frac{Z_a^2}{n_a^2} - \frac{Z_b^2}{n_b^2} \right) \right)^2 \quad (A2.31)$$

and

$$\Delta E = \frac{1}{2} \left(\frac{Z_a^2}{n_a^2} - \frac{Z_b^2}{n_b^2} \right). \quad (A2.32)$$

The principal quantum numbers are indicated by n_a and n_b for the respective nuclei A and B. The probability amplitude in eq. A2.30 is justified¹⁹

only when there is a one-to-one correspondence between the angle and impact parameter, in contrast to eq. A2.28.

APPENDIX 3

The computer program for the calculation of the differential cross section for the static potential in the eikonal phase, cf. Section 3.1, is listed.

```

//WATFIV JOB (522804028,DMB0S4N8),'S.R.ROGERS',TIME=(,59)
// EXEC WATFIV
//SYSIN DD *
$JOB ,TIME=(,59),PAGES=15
C COMPUTES DIFFERENTIAL CROSS SECTION FOR SCREENED COULOMB BRINKMAN -
C KRAMER'S APPROXIMATION FOR ELECTRON CAPTURE. INCLUDES EIKONAL
C PHASE AND CAPTURE PROBABILITY WORKED OUT IN THEORY BY STEVEN R.
C ROGERS AND JAMES H. MC GUIRE, KANSAS STATE UNIVERSITY.
C
C HYDROGEN (1S) TO HYDROGEN (1S) STATES
C
C IMPLICIT REAL*8(A-H,O-Z)
C REAL*8 MA,MB,NA,NB,KC,MU
C REAL*8 LAB
C COMMON COEF,XBAR,KC,THETA,RO,THETAD,ETA
C DIMENSION XW(100,10)
C EXTERNAL FOFY
C EXTERNAL GOFY
C PI=3.1415926535898
C ICRDER=12
C NUMBER=ICRDER/4
C
C READ IN GAUSS LEGENDRE WEIGHTS AND ABCISSA ARRAY, XW
C
C READ 10, ((XW(I,J),J=1,4),I=1,NUMBER)
C 10 FORMAT (4D20.14)
C
C READ IN INCIDENT ENERGY OF PROJECTILE IN ELECTRON VOLTS
C
C READ 1, EINC
C 1 FORMAT (D20.14)
C PRINT 3, EINC
C 3 FORMAT ('1',20X,'SCREENED COULOMB BRINKMAN KRAMERS APPROXIMATION'
C 1 //21X,'ENERGY (IN ELECTRON VOLTS)= ',1PD11.4/ )
C
C READ IN PROJECTILE(A)-TARGET(B) CHARGE AND MASS (ELECTRON MASS = 1)
C

```

```

C      READ 2, ZA,ZB,MA,MB
      2 FORMAT (4D20.14)

C      PRINCIPLE QUANTUM NUMBERS OF PROJECTILE-ELECTRON SYSTEM (NA) AND TARGET-
C      ELECTRON SYSTEM (NB)
C
      NB=1.
      NA=1.

C      ENERGY IN RYDBERGS
C
      RYDB=13.6D0
      EINC=EINC/RYDB

C      VO=(EINC/MA)**0.5D0
      MU=MA*MB/(MA+MB)
      KO=VO*MU
      ZABAR=ZA/NA
      ZBBAR=ZB/NB

C      LIMITS OF INTEGRATION FOR DIFFERENTIAL CROSS SECTIONS
C
      AA=1.D-10 /ZBBAR
      BB=.1D0 /ZBBAR
      CC=1. /ZBBAR
      DD=2. /ZBBAR
      EE=5. /ZBBAR
      FF=10. /ZBBAR

C      SBAR=VO/ ZRDAP*(1.-(ZBBAR**2-ZABAR**2)/VO**2)
      XBAR=ZBBAR*(1.+SBAR**2/4.)*.5D0
      C1=NA*32*PI*(ZBBAR*ZABAR)**2.5D0
      COEF=KO*C1/(16*VO*PI*XBAR**2)

C      AO IS THE RADIUS OF THE FIRST BOHR ORBIT, RO IS SCREENING PARAMETER
C
      AC=1.

```

```

RO=AO/2/ZB
PRINT 21, RO
21 FORMAT (' ', 20X, 'SCREENING RADIUS (IN AO) = ', 1PD11.4//)
PRINT 11, ZA, MA, NA, ZB, MB, NB
11 FORMAT (' ', 15X, 'CHARGE', 13X, 'MASS (ELECTRON MASS = 1)', 5X, 'PRINCI
1PLE QUANTUM NO.', 1X, 'PROJECTILE', 5X, 'ZA = ', F10.0, 4X, 'MA = ',
2F10.0, 4X, 'NA = ', F10.0//1X, 'TARGET', 9X, 'ZB = ', F10.0, 4X, 'MB = ',
3F10.0, 4X, 'NB = ', F10.0/)
BETA=(VO**4+2*VO**2*(ZBBAR**2+ZABAR**2)+(ZBBAR**2-ZABAR**2)**2)
1/(4*VO**2)
CLOSED=2**8*(ZA*ZB)**5/(5*VO**2*NA**3*NB**5*BETA**5)
C
C ETA=2.*ZA*ZB/VO
C THE NUCLEAR CHARGE OF THE NUCLEUS IS 1 FOR HYDROGEN.
C
ETA=2/VO
THETAM=0.
THETA=0.
THETAD=0.
SCBK=0.
ORKE=0.
TAU=0.
TAU=MA/MB
PRINT 101
101 FORMAT (' ', 8X, 'THETA', 20X, 'THETA', 21X, 'DIFFERENTIAL CROSS SECTIO
INS', 9X, 'RUNNING TOTAL CROSS SECTIONS', 6X, '(IN RADIANS)', 13X,
2'(IN DEGREES)', 21X, '(IN PI*AO**2/RADIAN)', 21X, '(IN PI*AO**2)')//
353X, 'BRINKMAN KRAMERS', 9X, 'SCREENED CCULEMB', 9X, 'B.K.', 9X, 'SCBK'//
42X, '(C.M.)', 7X, '(LAB)', 7X, '(C.M.)', 7X, '(LAB)', 7X, '(C.M.)',
57X, '(LAB)', 7X, '(C.M.)', 7X, '(LAB)', 7X, '(C.M.)', 7X, '(C.M.)')//
DO 50 ITER=1,50
THETAS=PI/1.D6
THETAM=THETA
C
C C OUTPUT SCALING TO COVER WIDEST RANGE OF VALUES OF ANGLE
C
IF (THETAD-2.D-2) 75,76,76

```

```

75 THETA=(THETA+THETAS)*1.3D0
   GO TO 77
76 THETAS=5.D-5
   IF (THETAD.GT.6.D-2) THETAS=THETAS*4.
   THETA=THETA+THETAS
77 THETAD=THETA*180.DD/PI
   LAB=(1.+2.*TAU*DCOS(THETA)+TAU**2)**1.5D0/DABS(1.+TAU*DCOS(THETA))
   THETA1=DARCCS((DCCS(THETA)+TAU)/(1.+2.*TAU*DCOS(THETA)+
1TAU**2)**1.5D0)
   THETA1=THETA1*180./PI
   UTHETA=THETA-THETA1
   A2=VC**2*((1.D0-(ZBBAR**2-ZABAR**2)/VC**2)**2+4*MU**2*THETA**2)/4
   HTHETA=C1*MU/(2.D0**5D0*PI*(ZBBAR**2+A2)**3)
   DQOBK=HTHETA**2
   DQOBKL=DQOBK*LAB
   GCBK=DQCBK*THETA*DTHETA
   CBK=QCBK+QOBK
   FOFY1=0.
   GOFY2=0.
   IF (THETAD.GT.0.3) GO TO 86
C
C FOFY IS THE REAL PART OF F(THETA)
C
C
C CALL SSIGMA (FOFY,AA,BB,CC,DD,EE,FF,5,XW,NUMBER,1,FOFY1)
C
C GOFY IS THE IMAGINARY PART OF F(THETA)
C
C CALL SSIGMA (GOFY,AA,BB,CC,DD,EE,FF,5,XW,NUMBER,2,GOFY2)
86 DIFCRS=(FOFY1**2+GOFY2**2)*2
   DIFCRL=DIFCRS*LAB
   SCPEEN=DIFCRS*THETA*DTHETA
   SCBK=SCBK+SCPEEN
   PRINT 22,THETA,THETA1,THETAD,THETA1,DQCBK,DQOBKL,DIFCRS,DIFCRL,
1CBK,SCBK
22 FORMAT (' ',1PD11.4,4(2X,1PD10.4,2X,1PD11.5),2X,1PD11.5)
   IF (THETAD.GE.2.) GO TO 51
50 CCNTINUE

```



```

CALL BESK (B/RO,0,BK0,IER0)
IF (IER0.NE.0) PRINT 7, IER0
7 FORMAT (' ',IER FOR BESK 0 IS ',I2)
CALL BESK (B/RO,1,BK1,IER1)
IF (IER1.NE.0) PRINT 10, IER1
10 FORMAT (' ',IER FOR BESK 1 IS ',I2)
CALL BESJ0 (KO*THETA*B,BJ,IER)
IF (IER.NE.0) PRINT 8, IER
8 FORMAT (' ',IER FOR BESJ IS ',I2)
GOFY=COEF*B**3*DCOS(ETA*(PK0+B/RO/2*BK1))*BK2*BJ
RETURN
END

```

```

SUBROUTINE BESK
COMPUTE THE K BESSEL FUNCTION FOR A GIVEN ARGUMENT AND ORDER
USAGE
CALL BESK(X,N,BK,IER)
DESCRIPTION OF PARAMETERS
X -THE ARGUMENT OF THE K BESSEL FUNCTION DESIRED
N -THE ORDER OF THE K BESSEL FUNCTION DESIRED
BK -THE RESULTANT K BESSEL FUNCTION
IER--RESULTANT ERROR CODE WHERE
IER=0 NO ERROR
IER=1 N IS NEGATIVE
IER=2 X IS ZERO OR NEGATIVE
IER=3 X.GT. 170, MACHINE RANGE EXCEEDED
IER=4 BK.GT. 10**70
REMARKS
N MUST BE GREATER THAN OR EQUAL TO ZERO
SUBROUTINES AND FUNCTION SUBPROGRAMS REQUIRED
NONE

```

```

BESK 40
BESK 50
BESK 60
BESK 70
BESK 80
BESK 90
BESK 100
BESK 110
BESK 120
BESK 130
BESK 140
BESK 150
BESK 160
BESK 170
BESK 180
BESK 190
BESK 200
BESK 210
BESK 220
BESK 230
BESK 240
BESK 250
BESK 260
BESK 270

```



```

C
C
C
      COMPUTE K0 USING POLYNOMIAL APPROXIMATION
27 G0=A*(1.2533141-.1566642*T(1)+.08911128*T(2)-.09139095*T(3)
  2+.1344596*T(4)-.2299850*T(5)+.3792410*T(6)-.5247277*T(7)
  3+.5575368*T(8)-.4262633*T(9)+.2184518*T(10)-.06680977*T(11)
  4+.009189383*T(12))*C
      IF(N)20,28,29
28 BK=G0
      RETURN
C
C
C
      COMPUTE K1 USING POLYNOMIAL APPROXIMATION
29 G1=A*(1.2533141+.4699927*T(1)-.1468583*T(2)+.1280427*T(3)
  2-.1736432*T(4)+.2847618*T(5)-.4594342*T(6)+.6283381*T(7)
  3-.6632295*T(8)+.5050239*T(9)-.2581304*T(10)+.07880001*T(11)
  4-.01082418*T(12))*C
      IF(N-1)20,30,31
30 BK=G1
      RETURN
C
C
C
      FROM KC,K1 COMPUTE KN USING RECURRENCE RELATION
31 DO 35 J=2,N
   GJ=2.*(DFLOAT(J)-1.)*G1/X+G0
   IF(GJ-1.0E70)33,33,32
32 IER=4
   GO TO 34
33 GO=G1
35 G1=GJ
34 BK=GJ
      RETURN
36 B=X/2.
   A=.5772157+DLGG(B)
   C=B*B
   IF(N-1)37,43,37
C

```

```

BESK 620
BESK 630
BESK 640
BESK 650
BESK 660
BESK 670
BESK 680
BESK 690
BESK 700
BESK 710
BESK 720
BESK 730
BESK 740
BESK 750
BESK 760
BESK 770
BESK 780
BESK 790
BESK 800
BESK 810
BESK 820
BESK 830
BESK 840
BESK 850
BESK 860
BESK 870
BESK 880
BESK 890
BESK 900
BESK 910
BESK 920
BESK 930
BESK 940
BESK 950
BESK 960
BESK 970
BESK 980

```

C CCOMPUTE K0 USING SERIES EXPANSION

```

C
37  GO=-A
    X2J=1.
    FACT=1.
    HJ=.0
    DO 40 J=1,6
      RJ=1./DFLOAT(J)
      X2J=X2J*C
      FACT=FACT*RJ*RJ
      HJ=HJ+RJ
40  GO=GO+X2J*FACT*(HJ-A)
    IF(N)43,42,43
42  BK=GO
    RETURN

```

C CCOMPUTE K1 USING SERIES EXPANSION

```

C
43  X2J=R
    FACT=1.
    HJ=1.
    G1=1./X+X2J*(.5+A-HJ)
    DO 50 J=2,8
      X2J=X2J*C
      RJ=1./DFLOAT(J)
      FACT=FACT*RJ*RJ
      HJ=HJ+RJ
50  G1=G1+X2J*FACT*(.5+(A-HJ)*DFLOAT(J))
    IF(N-1)31,52,31
52  BK=G1
    RETURN
    END

```

C SUBROUTINE BESJ0 (X,BJ,IER)

C COMPUTES THE J-ZERO BESSEL FUNCTION

C

C USAGE: CALL BESJ0 (X,BJ,IER)

C

BESK 990
 BESK1000
 BESK1010
 BESK1020
 BESK1030
 BESK1040
 BESK1050
 BESK1060
 BESK1070
 BESK1080
 BESK1090
 BESK1100
 BESK1110
 BESK1120
 BESK1130
 BESK1140
 BESK1150
 BESK1160
 BESK1170
 BESK1180
 BESK1190
 BESK1200
 BESK1210
 BESK1220
 BESK1230
 BESK1240
 BESK1250
 BESK1260
 BESK1270
 BESK1280
 BESK1290
 BESK1300


```

1+.00262573D0*(VALUE2)**3-.00054125D0*(VALUE2)**4-.00029333D0*
2(VALUE2)**5+.00013558D0*(VALUE2)**6
BJ=FD*DCOS(THETA0)/X**.5D0
RETURN
END

```

C	SUBROUTINE SSIGMA	SIGMA 01
C		SIGMA 02
C	COMPUTE THE INTEGRAL OF THE FUNCTION (Y) USING GAUSS	SIGMA 03
C	LEGENDRE INTEGRATION TECHNIQUE.	SIGMA 04
C		SIGMA 05
C	USAGE	SIGMA 06
C	CALL SSIGMA (FCFY,A,B,C,D,E,F,N,XW,NUMBER,INVERT,SSUM)	SIGMA 07
C		SIGMA 08
C	DESCRIPTION OF PARAMETERS	SIGMA 09
C	A-F ARE POINTS OF INTEGRATION	SIGMA 10
C	N- NUMBER OF INTERVALS TO INTEGRATE	SIGMA 11
C	XW - GAUSS LEGENDRE WEIGHTS AND ABSCISSA ARRAY	SIGMA 12
C	NUMBER - ORDER OF THE LEGENDRE POLYNOMIAL USED/4	SIGMA 13A
C	INVERT - SWITCHES THE FUNCTION IN THE INTEGRATION SUBROUTINE	SIGMA 13B
C	FROM FCFY (1) TO GCFY (2)	SIGMA 13C
C	SSUM - THE RESULTING INTEGRAL VALUE	SIGMA 13D
C		SIGMA 14
C	REMARKS	SIGMA 15
C	ORDER MUST BE DIVISIBLE BY 4	SIGMA 16
C		SIGMA 17
C	SUBROUTINES AND FUNCTION SUBPROGRAMS REQUIRED	SIGMA 18
C	DOUBLE PRECISION FUNCTION FCFY (Y)	SIGMA 19
C	IMPLICIT REAL*8(A-H,O-Z)	SIGMA 20
C	FCFY = FUNCTION TO BE INTEGRATED	SIGMA 21
C	RETURN	SIGMA 22
C	END	SIGMA 23
C		SIGMA 24
C	MUST PRECEDE MAIN PROGRAM	SIGMA 25
C	IMPLICIT REAL*8(A-H,O-Z)	SIGMA 26
C	DIMENSION XW(100,10)	SIGMA 27
C	EXTERNAL FCFY	SIGMA 28
C		SIGMA 29

```

C MUST PRECEDE SUBROUTINE SSIGMA
C   A-F,N, AND NUMBER
CC
CC   READ IN GAUSS LEGENDRE WEIGHTS AND ABCISSA ARRAY, XW
CC
CC   READ 10, ((XW(I,J),J=1,4),I=1,NUMBER)
C   10 FCRMAT (4D20.14)
C
C .....
SUBROUTINE SSIGMA (FOFY,AA,BB,C,D,E,F,N,XW,NUMBER,INVERT,SSUM)
IMPLICIT REAL*8(A-H,O-Z)
REAL*8 KO
COMMON COEF,XBAR,KC,THETA,RO,THETAD,ETA
DIMENSION XW(100,10)
A=AA
B=BB
SSUM=0.
N=0
30 N=N+1
NEG=1
40 I=0
50 DO 100 IX=1,NUMBER
J=-1
I=I+1
DO 100 JX=1,2
J=J+2
K=J+1
Y=(B-A)/2.D0*XW(I,J)*NEG+(B+A)/2.D0
IF (INVERT-1) 1,1,2
1 TOFY=FOFY(Y)
GO TO 3
2 TOFY=GOFY(Y)
3 CONTINUE
SUM=(B-A)/2.D0*XW(I,K)*TOFY
100 SSUM=SSUM+SUM
IF (NEG) 200,200,150
150 NEG=NEG-2

```

SIGMA 30
SIGMA 31
SIGMA 32
SIGMA 33
SIGMA34A
SIGMA34R
SIGMA34C
SIGMA34D
SIGMA35A
SIGMA35B
SIGMA35C

SIGMA35D

SIGMA 36
SIGMA 37
SIGMA 38
SIGMA 39
SIGMA 40
SIGMA 41
SIGMA 42
SIGMA 43
SIGMA 44
SIGMA 45
SIGMA 46
SIGMA47A
SIGMA47R
SIGMA47C
SIGMA47D
SIGMA47E
SIGMA47F
SIGMA 48
SIGMA 49
SIGMA 50
SIGMA 51

SIGMA 52
 SIGMA 53
 SIGMA 54
 SIGMA 56
 SIGMA 57
 SIGMA 58
 SIGMA 59
 SIGMA 60
 SIGMA 62
 SIGMA 63
 SIGMA 64
 SIGMA 65
 SIGMA 66
 SIGMA 68
 SIGMA 69
 SIGMA 70
 SIGMA 71
 SIGMA 72
 SIGMA 74
 SIGMA 75
 SIGMA 76
 SIGMA 77
 SIGMA 78
 SIGMA 80
 SIGMA 81

GO TO 40
 200 GO TO (220,270,320,370,420),M
 220 CCNTINUE
 IF (M-N) 260,420,420
 260 A=B
 B=C
 GO TO 30
 270 CCNTINUE
 IF (M-N) 310,420,420
 310 A=C
 B=D
 GO TO 30
 320 CCNTINUE
 IF (M-N) 360,420,420
 360 A=D
 B=E
 GO TO 30
 370 CCNTINUE
 IF (M-N) 410,420,420
 410 A=E
 B=F
 GO TO 30
 420 CCNTINUE
 RETURN
 END

\$ENTRY
 9.81560634246719E-014.71753363865118E-029.04117256370475E-011.06939325995318E-01
 7.69502674194305E-011.60078328543346E-015.87317954286617E-012.03167426723066E-01
 3.67831498958180E-012.33492536538355E-011.25233408511469E-012.49147045813403E-01
 50.
 E 3.
 1.00000000 E 00 1.000 E 00 1836. E 00 1836. E 00
 /*

APPENDIX 4

The main program for the Screened Coulomb Brinkman-Kramers approximation is listed, cf. Section 3.2. The three subroutines not listed are identical to those used in Appendix 3.

```

//WATFIV JOB (522304028,DMB0S4N8),'S.R.ROGERS',TIME=(,59)
// EXEC WATFIV
//SYSIN DD *
$JOB ,TIME=(,59),PAGES=15
C COMPUTES DIFFERENTIAL CROSS SECTION FOR SCREENED COULOMB BRINKMAN -
C KRAMER'S APPROXIMATION FOR ELECTRON CAPTURE. INCLUDES EIKONAL
C PHASE AND CAPTURE PROBABILITY WORKED OUT IN THEORY BY STEVEN R.
C ROGERS AND JAMES P. MC GUIRE, KANSAS STATE UNIVERSITY.
C
C ARGON (1S) TO HYDROGEN (1S) STATES
C
C IMPLICIT REAL*8(A-H,O-Z)
C REAL*8 MA,MD,NA,NB,KO,MU
C REAL*8 LAB
C COMMON COEF,XRAR,KO,THETA,RO,THETAD,ETA
C DIMENSION XW(100,10)
C EXTERNAL FOFY
C EXTERNAL GOFY
C PI=3.1415926535898
C IORDER=12
C NUMBER=10ORDER/4
C
C READ IN GAUSS LEGENDRE WEIGHTS AND ABCISSA ARRAY, XW
C
C READ 10, ((XW(I,J),J=1,4),I=1,NUMBER)
C 10 FORMAT (4D20.14)
C
C READ IN INCIDENT ENERGY OF PROJECTILE IN ELECTRON VOLTS
C
C READ 1, EINC
C 1 FORMAT (D20.14)
C PRINT 3, EINC
C 3 FORMAT ('1',20X,'SCREENED COULOMB BRINKMAN KRAMERS APPROXIMATION',
C 1 //21X,'ENERGY (IN ELECTRON VOLTS)= ',1PD11.4/ )
C
C READ IN PROJECTILE(A)-TARGET(B) CHARGE AND MASS (ELECTRON MASS = 1)
C

```

```

C      READ 2, ZA,ZB,MA,MB
C      2 FORMAT (4D20.14)
C
C PRINCIPLE QUANTUM NUMBERS OF PROJECTILE-ELECTRON SYSTEM (NA) AND TARGET-
C ELECTRON SYSTEM (NB)
C
C      NB=1.
C      NA=1.
C
C ENERGY IN RYDBERGS
C
C      RYDB=13.6D0
C      EINC=EINC/RYDB
C
C      VO=(EINC/MA)**0.5D0
C      MU=NA*NB/(MA+MB)
C      KC=VO*MU
C      ZAPAR=ZA/NA
C      ZBBAR=ZB/NB
C
C LIMITS OF INTEGRATION FOR DIFFERENTIAL CROSS SECTIONS
C
C      AA=1.D-10 /ZBBAR
C      BB=.1D0 /ZBBAR
C      CC=1. /ZBBAR
C      DD=2. /ZBBAR
C      EE=5. /ZBBAR
C      FF=1D. /ZBBAR
C
C      SBAR=VO/ ZBBAR*(1.-(ZBBAR**2-ZABAR**2)/VO**2)
C      XBAR=ZBBAR*(1.+SBAR**2/4.)**0.5D0
C      C1=NA**32*PI*(ZBBAR*ZABAR)**2.5D0
C      COEF=KO*C1/(16*VO*PI*XBAR**2)
C
C AO IS THE RADIUS OF THE FIRST BOHR ORBIT, RO IS SCREENING PARAMETER
C
C      AC=1.

```

```

RO=1.
RC=1.D-2
RC=1.D2
RC=AO/(ZA**(2.D0/3.D0)+ZB**(2.D0/3.D0))**.5D0
PRINT 21, RC
21 FORMAT (' ', 20X, 'SCREENING RADIUS (IN AO) = ', 1PD11.4//)
PRINT 11, ZA, MA, NA, ZB, MB, NB
11 FORMAT (' ', 15X, 'CHARGE', 13X, 'MASS (ELECTRON MASS = 1)', 5X, 'PRINCI
PLE QUANTUM NO.', // 1X, 'PROJECTILE', 5X, 'ZA = ', F10.0, 4X, 'MA = ',
2F10.0, 4X, 'NA = ', F10.0 // 1X, 'TARGET', 9X, 'ZB = ', F10.0, 4X, 'MB = ',
3F10.0, 4X, 'NB = ', F10.0 //)
BETA=(VO**4+2*VO**2*(ZBBAR**2+ZABAR**2)+(ZBBAR**2-ZABAR**2)**2)
1/(4*VO**2)
CLOSED=2**8*(ZA*ZB)**5/(5*VO**2*NA**3*NB**5*BETA**5)
ETA=2.*ZA*ZB/VO
THETAM=0.
THETA=0.
THETAD=0.
SCBK=0.
CBK=0.
TAU=0.
TAU=MA/MB
PRINT 101
101 FORMAT (' ', 8X, 'THETA', 20X, 'THETA', 21X, 'DIFFERENTIAL CROSS SECTIO
NS', 9X, 'RUNNING TOTAL CROSS SECTIONS', /6X, '(IN RADIANS)', 13X,
2'(IN DEGREES)', 21X, '(IN PI*AO**2/RADIAN)', 21X, '(IN PI*AO**2)', //
353X, 'BRINKMAN KRAMERS', 9X, 'SCREENED CCULOMB', 9X, 'B.K.', 9X, 'SCBK' //
42X, '(C.M.)', 7X, '(LAB)', 7X, '(C.M.)', 7X, '(LAB)', 7X, '(C.M.)',
57X, '(LAB)', 7X, '(C.M.)', 7X, '(LAB)', 7X, '(C.M.)', 7X, '(C.M.)' //)
DO 50 ITER=1, 50
THETAS=PI/1.D6
THETAM=THETA
C
C OUTPUT SCALING TO COVER WIDEST RANGE OF VALUES OF ANGLE
C
IF (THETAD-2.D-2) 75, 76, 76
75 THETA=(THETA+THETAS)*1.3D0

```

```

GO TO 77
76 THETAS=5.D-5
   IF (THETAD.GT.6.D-2) THETAS=THETAS*4.
   THETA=THETA+THETAS
77 THETAD=THETA*180.D0/PI
   LAB=(1.+2.*TAU*DCOS(THETA)+TAU**2)*#1.5D0/CABS(1.+TAU*DCOS(THETA))
   THETA1=DARCCS((DCOS(THETA)+TAU)/(1.+2.*TAU*DCOS(THETA))+
   ITAU**2)*#.5D0)
   THETD1=THETA1*180./PI
   DTHETA=THETA-THETAM
   A2=VD**2*(1.D0-(ZBBAR**2-ZABAR**2)/VC**2)*#2+4*MU**2*THETA**2)/4
   HTHETA=C1#MU/(2.D0**5D0*PI*(ZBBAR**2+A2)**3)
   DQCBK=HTHETA**2
   DQCBKL=DQCBK*LAB
   QCBK=DQCBK*THETA*OTHETA
   CBK=CBK+QCBK
   FOFY1=0.
   GOFY2=0.
   IF (THETAD.GT.0.3) GO TO 86
C
C FOFY IS THE REAL PART OF F(THETA)
C
C
C CALL SSIGMA (FOFY,AA,BB,CC,DD,EE,FF,5,XW,NUMBER,1,FOFY1)
C
C GOFY IS THE IMAGINARY PART OF F(THETA)
C
C CALL SSIGMA (GOFY,AA,BB,CC,DD,EE,FF,5,XW,NUMBER,2,GOFY2)
86 DIFCRS=(FOFY1**2+GOFY2**2)*2
   DIFCRL=DIFCRS*LAB
   SCREEN=DIFCRS*THETA*DTTHETA
   SCBK=SCBK+SCFEEN
   PRINT 22,THETA,THETA1,THETAD,THETD1,DQCBK,DQCBKL,DIFCRS,DIFCRL,
   1CBK,SCBK
22 FORMAT (' ',1PD11.4,4(2X,1PD10.4,2X,1PD11.5),2X,1PD11.5)
   IF (THETAD.GE.2.) GO TO 51
50 CONTINUE
51 PRINT 88

```

```

88 FORMAT ('0','TOTAL CROSS SECTIONS IN UNITS OF PI*AO**2')
PRINT 44, CLOSED,OBK,SCBK
44 FORMAT (' ','CLOSED FORM BK = ',1PD20.13,'; INTEGRAL VALUE BK = ',
11PD20.13,'; SCREENED CCULOMB BK = ',1PD20.13)
STOP
END

```

C
C SUBROUTINE FOR GETTING FUNCTION INTO INTEGRATION ROUTINE
C

```

DOUBLE PRECISION FUNCTION FCFY (B)
IMPLICIT REAL*8 (A-H,O-Z)
REAL*8 KO
COMMON COEF,XBAR,KO,THETA,RO,THETAD,ETA
CALL BESK (XBAR*B,2,BK2,IER2)
IF (IER2.NE.0) PRINT 6, IER2
6 FORMAT (' ','IER FOR BESK 2 IS ',I2)
CALL BESK (B/RO,0,BKO,IERO)
IF (IERO.NE.0) PRINT 7, IERO
7 FORMAT (' ','IER FOR BESK 0 IS ',I2)
CALL BESJO (KO*THETA*B,BJ,IER)
IF (IER.NE.0) PRINT 8, IER
8 FORMAT (' ','IER FOR BESJ IS ',I2)
FCFY=CGEF*B**3*DSIN (ETA *BK0)*BK2 *BJ
RETURN
END

```

C

```

DOUBLE PRECISION FUNCTION COFY (B)
IMPLICIT REAL*8 (A-H,O-Z)
REAL*8 KO
COMMON COEF,XBAR,KO,THETA,RO,THETAD,ETA
CALL BESK (XBAR*B,2,BK2,IER2)
IF (IER2.NE.0) PRINT 6, IER2
6 FORMAT (' ','IER FOR BESK 2 IS ',I2)
CALL BESK (B/RO,0,BKO,IERO)
IF (IERO.NE.0) PRINT 7, IERO
7 FORMAT (' ','IER FOR BESK 0 IS ',I2)
CALL BESJO (KO*THETA*B,BJ,IER)

```

```

IF (IER.NE.0) PRINT 8, IER
8 FORMAT (' ', IER FOR BESJ IS ',12)
GOFY=COEF#8**3*DCCS (ETA #BK0)*BK2 #8J
RETURN
END

```

```

C SUBROUTINE BESK BESK 40
C BESK 50
C

```

•

```

$ENTRY
9.81560634246719E-014.71753363865118E-029.04117256370475E-011.069393225995318E-01
7.69502674194305E-011.60078328543346E-015.87317954286617E-012.03167426723066E-01
3.67831498998130E-012.33492536538355E-011.25233408511469E-012.49147045813403E-01
6.0
E 6
1.00000000 E 00 18.00 E 00 1836. E 00 73440. E 00
/*

```

DIFFERENTIAL CROSS SECTIONS FOR CHARGE
TRANSFER USING SCREENED COULOMB POTENTIALS
IN THE EIKONAL APPROXIMATION

by

STEVEN RAY ROGERS

B.A., University of Northern Colorado, 1975

AN ABSTRACT OF A MASTER'S THESIS

submitted in partial fulfillment of the

requirements for the degree

MASTER OF SCIENCE

Department of Physics

KANSAS STATE UNIVERSITY

Manhattan, Kansas

1977

The effects of electronic screening of the internuclear potential in charge transfer is considered. By studying the differential cross section, the role of the internuclear potential is examined. Using the eikonal method of McCarroll and Salin (1968), the effective internuclear potential is represented by the static potential. The differential cross section for capture of K-shell electrons from helium by 293 keV protons observed by Bratton, et al., (1977), are compared with the theoretical predictions of Brinkman and Kramers (BK), Belkic and Salin (CBK), and myself (SBK). The shape of the observed differential cross section is in closer agreement to SBK, which uses the static potential, than BK, which uses no potential, or CBK, which uses the full Coulomb potential. The SBK differential cross section yields an improvement over CBK for the capture of K-shell electrons from argon by 6 MeV protons observed by Cocke, et al., (1976). Both CBK and SBK show marked improvements over BK.